Acknowledgements

Funding: This research did not receive any specific grant from funding agencies in the public, commercial, or not-for-profit sectors.

A hybrid robust-stochastic approach for strategic scheduling of a multi-energy system as a price-maker player in day-ahead wholesale market

Nima Nasiri[a], Saeed Zeynali[b], Sajad Najafi Ravadanegh[a], Mousa Marzband[b,c]

[a]*Electrical Engineering Department of Azarbaijan Shahid Madani University, Tabriz, Iran*
[b]*Northumbria University, Electrical Power and Control Systems Research Group, Ellison Place NE1 8ST, Newcastle upon Tyne, United Kingdom*
[c]*Center of Research Excellence in Renewable Energy and Power Systems, King Abdulaziz University, Jeddah 21589 Saudi Arabia*

Abstract

This study investigates the strategic scheduling of a multi-energy system (MES) in the day-ahead wholesale market (DWM) as a price-maker that can submit offers/bids to purchase/sell energy. In this regard, the proposed model presents a bi-level optimization problem, wherein the upper-level is the cost minimization objective of the MES, while the lower-level is considered as the wholesale market operator (WMO) that clears the market according to the received offers/bids from producers/consumers intending to maximize public satisfaction. The Karush-Kuhn-Tucker (KKT) conditions are utilized to convert the bi-level nonlinear problem into a single level mixed-integer linear problem (MILP). A combined heat and power (CHP) unit and wind turbines (WT) are integrated into MES as the production units, while various storage technologies, such as hydrogen energy storage (HES), natural gas storage (GS) and thermal energy storage (TES), as well as demand response program (DRP), are integrated to increase the flexibility of the system. A hybrid robust optimization (RO) and stochastic programming (SP) method is deployed to deal with uncertainties of MES. The results illustrate the efficacy of this model in manipulating market clearing price in favor of the MES, while different case studies show the privileges of utilizing a hybrid RO-SP method.

Email address: `s.najafi@azaruniv.ac.ir` `Corresponding author` (Sajad Najafi Ravadanegh)

Keywords: multi-energy systems; hydrogen energy storage; demand response programming; price-maker player; bi-level optimization; day-ahead wholesale market

---

Nomenclature

	Abbreviations
MES	Multi energy system
MESO	Multi energy system operator
DWM	Day ahead wholesale market
WMO	Wholesale market operator
GENCO	Generation company
TS	Transmission system
RO	Robust optimization
SP	Stochastic programming
CHP	Combined heat and power
EB	Electrical boiler
HES	Hydrogen energy storage
TES	Thermal energy storage
GS	Gas storage
DRP	Demand response programing
P2H	Power to hydrogen
H2P	Hydrogen to power
WT	Wind turbine
GAMS	General algebraic modeling system
LMP	locational market-clearing price in DWM
MILP	Mixed integer linear programing
	Indices
t, h, s	Indices of scheduling time, MES, uncertainty scenario
g, i	Indices of GENCO, power system bus

A_i^g	Set of GENCO connected to the power system bus i
A_i^h	Set of MES connected to the power system bus i
Tr	Set of power transmission lines
	Parameters
$P_i^{A,B,C,D}$	Electrical operational points of CHP
$H_i^{A,B,C,D}$	Thermal operational points of CHP
$C_{h,t}^g$	Price of natural gas purchased by MESO ($/Kcfh)
C_h^{P2H}	Price of the P2H convert in HES ($/MWh)
C_h^{up}/C_h^{dn}	Price of shift up/shift down in DRP ($/MWh)
P_h^{Max}/P_h^{Min}	Maximum / minimum output electricity power of CHP unit in MES h (MW)
H_h^{Max}/H_h^{Min}	Maximum / minimum output thermal power of CHP unit in MES h (MW)
R_h^{up}/R_h^{dn}	Up/ down ramp rate limit of CHP unit in MES h (MW)
T_h^{Ue}/T_h^{De}	Minimum Up/ down time of CHP unit in MES h (h)
C_h^{SU}/C_h^{SD}	Startup/ shutdown fuel consumption of CHP unit in MES h (Kcf)
$\eta_h^{P2H}/\eta_h^{H2P}$	Stored/ generated hydrogen efficiencies of HES in MES h (%)
η_h^{ch}/η_h^{dis}	Charge/ discharge efficiencies of TES in MES h (%)
$\eta_h^{GSS,ch}/\eta_h^{GSS,dis}$	Charge / discharge efficiencies of GS in MES h (%)
A_h^{Max}/A_h^{Min}	Maximum/ minimum storage capacity of HES in MES h (MW)
B_h^{Max}/B_h^{Min}	Maximum/ minimum storage capacity of TES in MES h (MW)
GS_h^{Max}/GS_h^{Min}	Maximum/ minimum storage capacity of GS in MES h (Kcf)
$P_{h,Max}^{P2H}/P_{h,Min}^{P2H}$	Maximum/ minimum stored hydrogen in HES in MES h (MW)
$P_{h,Max}^{H2P}/P_{h,Min}^{H2P}$	Maximum/ minimum generated hydrogen in HES in MES h (MW)
$H_{h,Max}^{ch}/H_{h,Max}^{dis}$	Maximum charge/ discharge of TES in MES h (MW)
$GS_h^{ch,max}/GS_h^{dis,max}$	Maximum charge/ discharge of GS in MES h (KCf)
LPF	Shift load factor of DRP in MES (%)

$P^{D}_{h,s,t}/H^{D}_{h,s,t}/G^{D}_{h,s,t}$	Electricity/ heating/ gas demand of MES h in scenario s at period t
η^{EB}_{h}	Efficiencies of EB in MES h (%)
LPF	Load profile factor in DRP
$P^{EB,max}_{h}$	Maximum power limit of EB in MES h (MW)
$P^{Wind\_max}_{h,t}$	Maximum power limit of WT in MES h (MW)
η^{CHP}_{h}	Efficiencies of CHP unit in MES h (%)
C^{G}_{g}	Offered price of the GENCO g in WM ($/MWh)
$P^{d}_{i,t}$	Electricity demand of TS in bus i at period t
$P^{GMax}_{g,t}$	Maximum power limit of GENCO g in period t (MW)
$P^{EH,Max}_{h}/P^{EH,Min}_{h}$	Maximum/ minimum power exchanged between MES h and WM (MW)
$C^{Max}_{i,j}$	Maximum capacity electricity power flow in TS lines (i,j) (MW)
Γ	Budget uncertainty
	Variables
$P^{EH}_{h,t}$	Electricity purchase/sell of MES in DWM (MW)
$G^{EH}_{h,t,s}$	Natural gas purchased by MES (kcf)
$\lambda^{e}_{i,t}$	Wholesale market clearing price in bus i at period t ($/MWh)
$C^{EH}_{h,t}$	Offer/bid MES h in the DWM at period t
$P^{CHP}_{h,s,t}$	Output electricity power of CHP unit in MES h at scenario s and period t
$H^{CHP}_{h,s,t}$	Output heating power of CHP unit in MES h at scenario s and period t
$SU_{h,s,t}/SD_{h,s,t}$	Startup/ shutdown of fuel consumed by the CHP unit in MES h at scenario s and period t
$A^{HES}_{h,s,t}$	Hydrogen storage capacity of hydrogen storage tank in MES h at scenario s and period t
$P^{P2H}_{h,s,t}/P^{H2P}_{h,s,t}$	Generated / Stored hydrogen of HES in MES h at scenario s and period t
$MI_{h,s,t}$	Other consumers of hydrogen energy in MES h at scenario s and period t

$B^{HSS}_{h,s,t}$	Thermal storage capacity of thermal storage tank in MES h at scenario s and period t
$H^{ch}_{h,s,t}/H^{dis}_{h,s,t}$	Charge/discharge of TES in MES h at scenario s and period t
$GS^{GSS}_{h,s,t}$	Natural gas storage capacity of Gas storage tank in MES h at scenario s and period t
$G^{ch}_{h,s,t}/G^{ch}_{h,s,t}$	Charge/ discharge of GS in MES h at scenario s and period t
$DR^{up}_{h,s,t}/DR^{dn}_{h,s,t}$	Change the electric demand after applying the DRP in MES h at scenario s and period t
$P^{DR}_{h,s,t}$	Shifted electric load in MES h at scenario s and period t
$H^{EB}_{h,t,s}$	Thermal output power of the EB in MES h at scenario s and period t
$P^{EB}_{h,t,s}$	Electric power consumed by the EB in MES h at scenario s and period t
$P^{Wind}_{h,s,t}$	Output power of WT in MES h at scenario s and period t
$y^{RO}_{h,s,t}, p^{RO}_{h,s,t}, z^{RO}_{h,s,t}$	Dual variables related to robust optimization in MES h at scenario s and period t
$\delta_{i,t}$	Bus's voltage angle of TS at period t
$\mu/\nu/\zeta$	Dual variables related to bi-level optimization
	Binary variables
$I_{h,s,t}$	Commitment status of CHP unit in MES h at scenario s and period t
$Y_{h,t}/Z_{h,t}$	Startup/ shutdown status of CHP unit in MES h at scenario s and period t
$I^{P2H}_{h,s,t}/I^{H2P}_{h,s,t}$	Generated/ Stored status of HES in MES h at scenario s and period t

1. Introduction

1.1. Motivation

Scattering distribution and energy storage units, as opposed to centralizing at large scales, has proven to be far more advantageous [1]. As a result, more and more private companies are investing in dispersed generation and storage technologies [2]. This new trend has laid the foundations of the free energy market, which is fair, efficient, reliable and competitive unlike the monopolistic market [3]. In

this respect, multi-energy systems (MESs) are playing an essential role. An MES usually consists of multiple generation and storage units, which should be optimally scheduled to provide energy with minimal cost [4]. Moreover, the MES is able to participate in the day-ahead wholesale market (DWM) as a price-maker player that can exert influence on locational market-clearing (LMP) of the transmission system (TS) by submitting offers/bids to purchase/sell energy [5]. The problem, however, is that the wholesale market operator (WMO) clears the market to maximize social welfare, which is in contrast with the cost objective of the MES. Therefore, a bi-level optimization framework offers a workable solution for this conundrum, wherein the upper and lower levels are MES and WMO objectives, respectively. This type of problem offers the best tradeoff equilibrium for both WMO and MES [6]. The combined heat and power (CHP) units are particularly attractive alternatives for MESs [7], as they can satisfy thermal and electrical loads simultaneously, and by recycling the dissipated thermal energy, the efficiency of the CHP units can be as much as 90%, while in comparison to the thermal units and boilers, the CHPs can save up 10 to 40 percent of the fuel [8], [9].

Additionally, the energy storage systems have the most pivotal role in MES as they provide elasticity, which is considered as the trump card of the MES against inherent uncertainties. An energy storage system can identify the patterns in price, production or consumption volatilities and deploy them to manipulate LMP in favor of the MES [10]. Additionally, by order of the 784th federal energy regulatory commission (FERC), the participation of the energy storage systems in energy markets has been facilitated and multiple financial incentives (e.g., tax exemption and clean production credits) are provided for keen investors [11]. However, considering the fast dynamics of electrical energy, the efforts are hampered by rudimentary predicaments, such as hefty price tag, high power loss and insufficient space [12]. On the other hand, fluids such as hydrogen and natural gas have slower dynamics and higher compressibility factor; hence they can be stored in massive scales up to hundreds of megawatts. Hydrogen, as a particularly green type of energy, has been the focal point for many researchers [13]. That said, the effectiveness of hydrogen energy storage (HES) and natural gas storage (GS) in MES and their strategic be-

havior in energy markets are under-researched subjects. Furthermore, a demand response program (DRP) can be as effective as a storage unit in shifting demand to off-peak time intervals and increasing profit [14]. The flexibility of thermal loads can be increased by a thermal energy storage (TES), while electrical boiler is an effective way of converting spillage of renewable energies into thermal energy [15].

1.2. Literature review

There have been numerous studies focused on various facets of MES, such as planning [16], reliability [17], resilience [18], energy management methods [19] and handling of uncertainties [20]. In fact, the behavior of the MES in different energy markets has been the point of contention in recent studies. A strategic bidding strategy has been scrutinized in [21] for MES in both day-ahead and real-time markets. In a similar study [22], the researchers evaluate the possibility of utilizing two-stage stochastic programming to participate in real-time and day-ahead markets as a multi-energy system operator (MESO). Furthermore, the authors in [23] evaluated the participation of MES in the reserve market together with DWM. Ref [24] proposed a bi-level optimization framework, wherein MESO participates in a retail-market. The strategic units' participation in DWM was addressed in [25] considering high wind power penetration with stochastic scenarios. The bidding curve of microgrids in ancillary service market is addressed in [26] utilizing real-world data. A bidding strategy approach has been proposed by [27] for a price-maker MESO that has the objective of maximizing profit in the presence of other MESs. The authors in [28] provide deep insight into optimal scheduling of MES when conducting transactions with pool-market, forward contracts and natural gas market. The study effectively incorporates an SP-based bi-level optimization method. Moreover, the functionality of the power-to-X storage technologies in MES was addressed in [29]. Green carbon credits have also been an important research topic. In this respect, [30] evaluates the impact of green credits in strategic market environment.

A mathematical programming approach with equilibrium constraints has been investigated in [31] to study the profit-oriented behavior of the MESO in electricity and thermal energy markets, in which the submitted offers/bids are scheduled

in the upper-level, while the lower-level corresponds to clearing integrated thermal and electrical markets. An iterative two-step optimization framework has been suggested in [32] for optimal participation of MESO in wholesale electricity and natural gas markets, wherein the upper-level and lower-level problems are optimal scheduling of MES and DWM-clearing, respectively. To investigate the behavior of MES players and local energy systems in trade ties with wholesale market and retail market, a bi-level framework has been reported in [33]. In an analogous study [34], the authors have presented a hierarchical tri-level optimization framework, in which the upper-level problem is the maximization of the MES's profit, while the lower-level problems are consecutively the maximization of the local energy system's profit and social welfare. To investigate the transactions of the transmission networks with MES, a bi-level optimization framework has been investigated in [35]. The upper-level problem is the minimization of the total operations cost of TS, while the lower-level corresponds to the total operation cost of multiple MESs. The authors in [36] have studied the functionality of distributed energy resource aggregator as a participant in the real-time market. The study utilizes a risk-based bi-level framework, wherein the upper and lower level problems are respectively the optimal scheduling of the MES and market clearing process. Ref [37] has proposed a RO framework to minimize the operational costs of MES considering the fluctuations in wind power. A hybrid RO-SP method has been deployed in [38] to investigate the ways in which an MESO can participate in hydrogen and natural gas markets utilizing hydrogen to power (H2P) technology. A strategic real-time and wholesale market bidding technique has been reported in [39] to optimize the bidding strategy of a microgrid that is equipped with HES and DRP. The same authors developed their model to include the reserve market in [40]. The authors in [41] proposed a bi-level optimization framework for profit-oriented P2H unit from technical constraints and market point of view. The offers/bids of the P2H unit make up the upper-level problem, while the lower-level consists of the market clearing process.

1.3. Contributions

All of the reviewed studies have made significant discoveries and contributions in various aspects. That said, none of them have investigated the strategic scheduling of MES with a hybrid RO-SP method as a price-maker player in DWM using a bi-level optimization approach. In this concern, the main gaps in previous studies can be outlined as follows:

1. Studies including [16–24, 28, 32–35, 37–39, 41] have focused on strategically scheduling MES as a price-taker player. However, a price-taker player must be a function of the market and cannot influence the market clearing price.
2. The publications in [16–24, 27, 28, 33, 34, 37–39] have proposed diverse methods to strategically schedule MES in DWM. Nevertheless, all of them have ignored the presence of the power system and its constraints. In addition, including a power system model is imperative, as market-clearing price is calculated according to the system's limitation and line congestion.
3. Although refs [16–36] have addressed the integration of various storage and responsive load technologies in MES, they have not addressed the presence of HES and DRP in a price-maker MES. However, these types of model can be notably more lucrative, as MES can utilize HES and DRP to manipulate LMP, which leads to more profit.

This paper proposes an unique bi-level optimization framework to inspect the strategic scheduling of an MES in DWM as a price-maker player with HES and DRP. In the upper-level problem, the MES strategically submits offers/bids and schedules HES and other components to minimize total operational cost. At the lower-level, WMO receives all the offers/bids from producers/consumers while clearing the DWM to maximize public satisfaction. Load consumption usually follows a specific probability distribution. For this reason, thermal demand, natural gas demand and electrical demand are modelled as stochastic scenarios. On the other hand, the wind energy has a more arbitrary nature. Therefore, a robust optimization framework is deployed to model wind power uncertainty and increase systems robustness on the production side, which enables the operator to strike a balance between risk and profit. Moreover, the results are validated with IEEE 6-bus and IEEE 24-bus

test systems. Overall, the main contributions of this study can be emphasized as follows:

1. A novel bi-level optimization framework is introduced to evaluate the strategic behavior of the MES as a price-maker in DWM.
2. The impact of coordinated scheduling of HES and DRP is evaluated for the price-maker MES, while it is illustrated how they can manipulate LMP in favor of the MES.
3. A hybrid RO-SP method is utilized to handle intermittent natures, and its impact on LMP is investigated

2. Problem Description

The overall visual representation of the proposed MES can be observed in Figure 1. As illustrated, the proposed MES consists of various apparatus, e.g., CHP unit, TES, GS, HES, EB and WT. All of which are managed by an administrative entity known as MESO. The main concept is to recover the wind energy spillage through various storage technologies and DRP. The hydrogen is obtained through the power to hydrogen (P2H) technology, then stored in HES and converted back to electricity using hydrogen to power (H2P) technology. The duties of MESO consist of executing DRP, handling uncertainties, participating in DWM, scheduling and monitoring equipment. Figure 2 provides a flowchart of the way in which MES participates in DWM and interacts with WMO as a price-setter player. Initially, the MESO collect the available equipment data, such as production capacity of the CHP units, predicted interval of wind power production, HES's capacity, the capacity of EB and stochastic load scenarios. Subsequently, the MESO submits optimal offers/bids to WMO, where the WMO receives all offers from wholesale producers, such as GENCOs and bids from consumers while clearing the DWM to maximize social welfare. Nevertheless, this process is carried out delicately under the restrictions of GENCOs and TS, which are imposed by transmission system operator (TSO). The production of the GENCO's, the customer energy consumption, and the amount of power exchanged by MES is calculated at the market clearing process. If the obtained results

are not favorable to MES, the MESO can submit different bids and evaluate the new outcome. This procedure is continued until reaching an equilibrium point in which both WMO and MESO are satisfied. In this study, this so-called equilibrium point is reached by turning the bi-level nonlinear problem into a linear single-level problem via the KKT conditions. Without the loss of generality, the WMO decisions and MES decisions have mutual implications for each side. Therefore, it is essential to create the optimal response model of WMO for MES as it can schedule the units considering the relative response of the market.

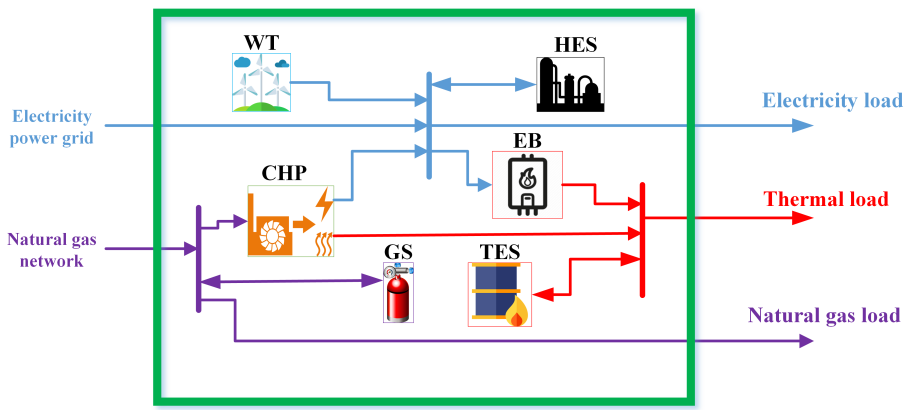

Figure 1: Structure of the proposed MES

3. Formulation

3.1. Multi-energy system (Upper-level problem)

3.1.1. Objective functions

The core objective of the upper-level is to minimize the MES operational cost as defined in Eq. (1). The first term is the cost of energy bought from DWM, the second and third terms represent the cost of importing energy from the natural gas network and the charging cost of the HES [42], respectively. Finally, the last two terms represent the cost of deploying DRP.

$$\min \sum_{s} \pi_s \left\{ \sum_{t} \sum_{h} \left[\begin{array}{l} \lambda^{e}_{i,t} P^{EH}_{h,t} + C^{g}_{h,t} G^{EH}_{h,t,s} + C^{P2H}_{h} P^{P2H}_{h,t,s} \\ +(C^{dn}_{h} DR^{dn}_{h,s,t} + C^{up}_{h} DR^{up}_{h,s,t}) \end{array} \right] \right\} \tag{1}$$

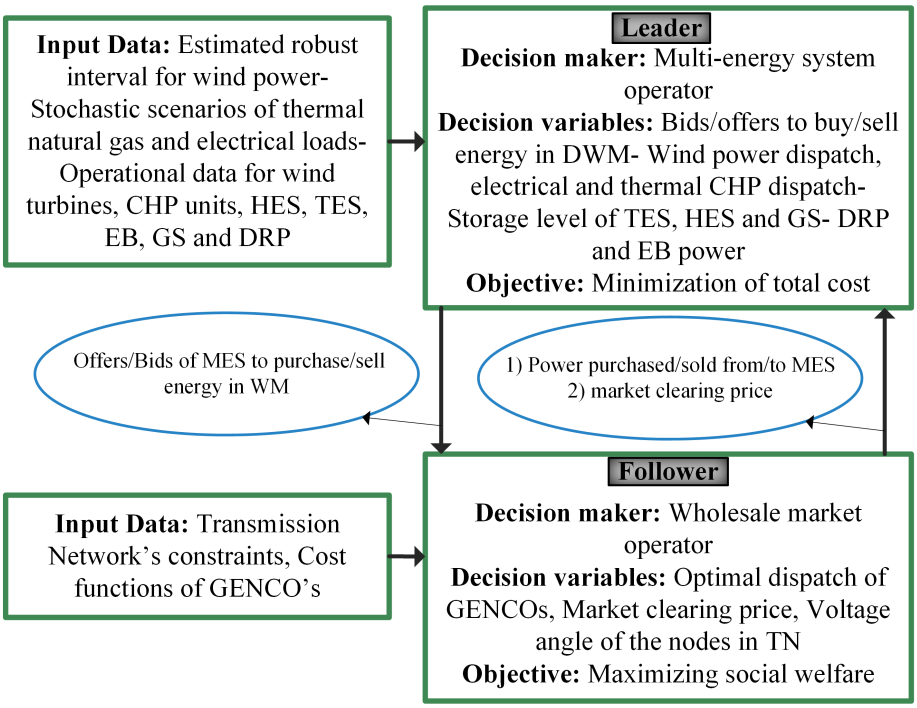

Figure 2: The transaction algorithm between MESO and WMO

3.1.2. The combined heat and power unit (CHP)

As it can be observed from Figure 3, the thermal and electrical output of the CHP unit are strictly intertwined and limited to the feasible operation region (FOR). Equations Eqs. (2)-(6) embody the mathematical implementation of FOR. Eqs. (2)-(3) impose the electrical and thermal power generation limits of the CHPs. Eq. (4) define the area under the line A-B, while Eq. (5) model the upper area of the line B-C. It can be seen that when $I_{h,t,s}$ is zero, the electrical and thermal output of the CHP unit will be zero. Moreover, Eq. (6) enforces the area limit above line C-D. The ramp-up/ramp-down rate of rates of the CHP are derived in Eqs. (7)-(8), while the binary equation Eq. (9) determines the on/off status of the CHP. To prevent the CHP unit from being on and off at the same time, equation Eq. (10) is imposed. To clarify the initial and final hours of the scheduling horizon in minimum on-time/off-time constraints, the auxiliary constants in Eqs. (11)-(12) are

utilized. Eq. (13) declares the minimum required on-time to start the CHP unit up. The on-time for all time steps, except the initial and final periods, is imposed by Eq. (14). Moreover, Eq. (15) defines the on-time for final operational hours. Similarly, the minimum off-time constraint is established in Eq. (16) to shut the CHP unit down. The minimum off-time in all hours except the initial and final ones is defined by Eq. (17), while Eq. (18) enforces the minimum off-time in final time intervals. Eventually, Eqs. (19)-(20) determine the amount of fuel that is required to turn the CHP unit on or off [43].

$$P_h^{Min} I_{h,s,t} \leqslant P_{h,s,t}^{CHP} \leqslant P_h^{Max} I_{h,s,t} \quad \forall h, \forall s, \forall t \tag{2}$$

$$0 \leqslant H_{h,s,t}^{CHP} \leqslant H_h^A I_{h,s,t} \quad \forall h, \forall s, \forall t \tag{3}$$

$$P_{h,s,t}^{CHP} - P_h^A - \frac{P_h^A - P_h^B}{H_h^A - H_h^B}(H_{h,t,s}^{CHP} - H_h^A) \leqslant 0 \quad \forall h, \forall s, \forall t \tag{4}$$

$$P_{h,s,t}^{CHP} - P_h^B - \frac{P_h^B - P_h^C}{H_h^B - H_h^C}(H_{h,s,t}^{CHP} - H_h^B) \geqslant -(1 - I_{h,t,s})M \quad \forall h, \forall s, \forall t \tag{5}$$

$$P_{h,s,t}^{CHP} - P_h^C - \frac{P_h^C - P_h^D}{H_h^C - H_h^D}(H_{h,s,t}^{CHP} - H_h^C) \geqslant -(1 - I_{h,t,s})M \quad \forall h, \forall s, \forall t \tag{6}$$

$$P_{h,s,t}^{CHP} - P_{h,s,t-1}^{CHP} \leqslant [1 - Y_{h,t,s}]\, R_h^{up} + Y_{h,t,s} P_h^{min} \quad \forall h, \forall s, \forall t \tag{7}$$

$$P_{h,s,t-1}^{CHP} - P_{h,s,t}^{CHP} \leqslant [1 - Z_{h,s,t}]\, R_h^{dn} + Z_{h,s,t} P_h^{min} \quad \forall h, \forall s, \forall t \tag{8}$$

$$Y_{h,s,t} - Z_{h,s,t} = I_{h,s,t-1} - I_{h,s,t} \quad \forall h, \forall s, \forall t \tag{9}$$

$$Y_{h,s,t} + Z_{h,s,t} \leqslant 1 \quad \forall h, \forall s, \forall t \tag{10}$$

$$T_h^{Ue} = \min\left\{T, (T^{Ue} - T_h^{U0}) I_{h,t=0,s}\right\} \quad \forall s, \forall h \tag{11}$$

$$T_h^{De} = \min\left\{T, (T^{De} - T_h^{U0})(1 - I_{h,t=0,s})\right\} \quad \forall s, \forall h \tag{12}$$

$$\sum_{t=1}^{T_h^{Ue}} I_{h,s,t} = T_h^{Ue} \quad \forall h, \forall s \tag{13}$$

$$\sum_{t=r}^{t+T_h^{Ue}-1} I_{h,s,r} \geqslant T_h^{Ue} y_{h,s,t} \quad \forall h, \forall s, \forall t = \left[T_h^{Ue} + 1, ..., T - T_h^{U} + 1\right] \tag{14}$$

$$\sum_{t=r}^{T} (I_{h,s,r} - y_{h,s,t}) \geqslant 0 \quad \forall h, \forall s, \forall t = \left[T - T_h^{Ue} + 2, ..., T\right] \tag{15}$$

$$\sum_{t=1}^{T_h^{De}} I_{h,s,t} = 0 \quad \forall h, \forall s \tag{16}$$

$$\sum_{t=r}^{t+T_h^{De}-1} (1 - I_{h,s,r}) \geqslant T_h^{De} z_{h,s,t} \quad \forall h, \forall s, \forall t = \left[T_h^{De} + 1, ..., T - T_h^{D} + 1\right] \tag{17}$$

$$\sum_{t=r}^{T} (1 - I_{h,s,r} - z_{h,t}) \geqslant 0 \quad \forall h, \forall s, \forall t = \left[T - T_h^{De} + 2, ..., T\right] \tag{18}$$

$$SU_{h,s,t} \geqslant C_h^{SU} Y_{h,s,t} \quad \forall h, \forall s, \forall t \tag{19}$$

$$SD_{h,s,t} \geqslant C_h^{SD} Z_{h,s,t} \quad \forall h, \forall s, \forall t \tag{20}$$

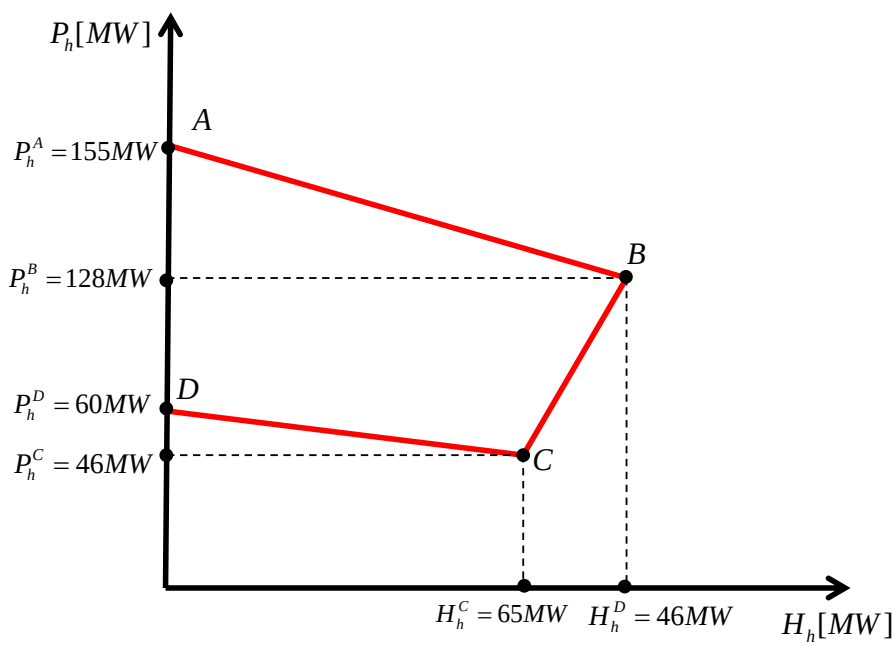

Figure 3: FOR region of the CHP unit

3.1.3. *Hydrogen energy storage (HES)*

The HES model is established by Eqs. (21)-(27), wherein Eq. (21) defines the amount of hydrogen in the storage, while Eqs. (22)-(23)define the upper and the lower boundaries of the storage capacity. Equation Eq. (24) limits the hydrogen consumption of the industrial consumers (assumed to be zero in this study). Equations

Eqs. (25)-(26) respectively define the maximum and minimum charge/discharge limitations. At last, Eq. (27) restrains simultaneous charge/discharge [44].

$$A^{HES}_{h,s,t} = A^{HES}_{h,s,t-1} + \eta^{P2H}_{h} P^{P2H}_{h,s,t} - \frac{P^{H2P}_{h,s,t}}{\eta^{H2P}_{h}} - MI_{h,s,t} \quad \forall h, \forall t, \forall s \tag{21}$$

$$A^{Min}_{h} \leqslant A^{HES}_{h,s,t} \leqslant A^{Max}_{h} \quad \forall h, \forall t, \forall s \tag{22}$$

$$A^{HES}_{h,s,t=1} = A^{HES}_{h,s,t=24} \quad \forall h, \forall s \tag{23}$$

$$0 \leqslant MI_{h,s,t} \leqslant MI^{Max}_{h} \quad \forall h, \forall t, \forall s \tag{24}$$

$$P^{P2H}_{h,Min} I^{P2H}_{h,s,t} \leqslant P^{P2H}_{h,s,t} \leqslant P^{P2H}_{h,Max} I^{P2H}_{h,s,t} \quad \forall h, \forall t, \forall s \tag{25}$$

$$P^{H2P}_{h,Min} I^{H2P}_{h,s,t} \leqslant P^{H2P}_{h,s,t} \leqslant P^{H2P}_{h,Max} I^{H2P}_{h,s,t} \quad \forall h, \forall t, \forall s \tag{26}$$

$$I^{P2H}_{h,s,t} + I^{H2P}_{h,s,t} \leqslant 1 \quad \forall h, \forall t, \forall s \tag{27}$$

3.1.4. Thermal energy storage (TES)

The mathematical model of the TES is appointed to Eqs. (28)-(32), wherein Eq. (28) describes the amount of stored energy. Eqs. (29)-(31) enforce the capacity and rate limits, while the initial and final amount of stored energy is equalized in Eq. (32) [45].

$$B^{HSS}_{h,s,t} = B^{HSS}_{h,s,t-1} + \eta^{ch}_{h} H^{ch}_{h,s,t} - \frac{H^{dis}_{h,s,t}}{\eta^{dis}_{h}} \quad \forall h, \forall t, \forall s \tag{28}$$

$$B^{Min}_{h} \leqslant B^{HSS}_{h,s,t} \leqslant B^{Max}_{h} \quad \forall h, \forall t, \forall s \tag{29}$$

$$0 \leqslant H^{dis}_{h,s,t} \leqslant H^{dis}_{h,Max} \quad \forall h, \forall s \tag{30}$$

$$0 \leqslant H^{ch}_{h,s,t} \leqslant H^{ch}_{h,Max} \quad \forall h, \forall t, \forall s \tag{31}$$

$$B^{HSS}_{h,s,t=1} = B^{HSS}_{h,s,t=24} \quad \forall h, \forall t, \forall s \tag{32}$$

3.1.5. Natural gas storage (NGS)

The amount of stored natural gas in each time interval is established via Eq. (33), whilst Eqs. (34)-(36) confine the charge/discharge rates and the amount of stored natural gas within the nominal values. Similar to the other storage units, the initial and final storage states are equalized via Eq. (37).

$$GS^{GSS}_{h,s,t} = GS^{GSS}_{h,s,t-1} + \eta^{GSS,ch}_{h} G^{ch}_{h,s,t} - \frac{G^{dis}_{h,s,t}}{\eta^{GSS,dis}_{h}} \quad \forall h, \forall s, \forall t \tag{33}$$

$$0 \leqslant G^{ch}_{h,s,t} \leqslant GS^{ch,max}_{h} \quad \forall h, \forall s, \forall t \tag{34}$$

$$0 \leqslant GS^{dis}_{h,s,t} \leqslant GS^{dis,max}_{h} \quad \forall h, \forall s, \forall t \tag{35}$$

$$GS^{Min}_{h} \leqslant GS^{GSS}_{h,s,t} \leqslant GS^{Max}_{h} \quad \forall h, \forall s, \forall t \tag{36}$$

$$GS_{h,s,t=0} = GS_{h,s,t=24} \quad \forall h, \forall s, \forall t \tag{37}$$

3.1.6. Demand response program (DRP)

The DRP is expressed by equations Eqs. (38)-(41). The upward and downward shift in load value is assigned to Eqs. (38)-(39), while Eq. (40) indicates that the amount of shift in either direction is equal. Eq. (41) is designated for the ultimate load demand after applying DRP, which is utilized in the electrical equilibrium equation of the MES.

$$0 \leqslant DR^{up}_{h,s,t} \leqslant LPF.P^{d}_{h,s,t} \quad \forall h, \forall s, \forall t \tag{38}$$

$$0 \leqslant DR^{dn}_{h,s,t} \leqslant LPF.P^{d}_{h,s,t} \quad \forall h, \forall s, \forall t \tag{39}$$

$$\sum_{t} DR^{dn}_{h,s,t} = \sum_{t} DR^{up}_{h,s,t} \quad \forall h, \forall s, \forall t \tag{40}$$

$$P^{DR}_{h,s,t} = P^{d}_{h,s,t} - DR^{dn}_{h,s,t} + DR^{up}_{h,s,t} \quad \forall h, \forall s, \forall t \tag{41}$$

3.1.7. Electrical boiler (EB)

The main concept behind EB is to convert overproduction of the wind power to thermal energy that would otherwise have been spilled. Therefore, using EB leads to improved system flexibility in satisfying thermal loads while supporting the CHP unit in peak hours. The transformation of electrical energy into thermal energy is indicated by Eq. (42) and its limits are enforced by Eq. (43).

$$H^{EB}_{h,s,t} = \eta^{EB}_{h} P^{EB}_{h,s,t} \quad \forall h, \forall s, \forall t \tag{42}$$

$$0 \leqslant P^{EB}_{h,s,t} \leqslant P^{EB,max}_{h} \quad \forall h, \forall s, \forall t \tag{43}$$

3.1.8. Robust wind power model

The wind power uncertainty is one of the chief predicaments faced by MES. However, the MESO can have some rough estimates about the variation interval of the wind power. Therefore, a RO method is deployed in this study to make the system more reliable against the wind power unpredictability. The deterministic wind power model is established via Eq. (44) and the linear robust formulation is defined by Eqs. (45)-(48). The mathematical proof of this robust formulation can be found in [46], and further information on the hybrid RO-SP method is included in Appendix A.

$$0 \leqslant P^{Wind}_{h,s,t} \leqslant P^{Wind\_max}_{h,t} \quad \forall h, \forall s, \forall t \tag{44}$$

$$P^{Wind}_{h,s,t} - x^{RO}_{h,s,t} P^{Wind\_max}_{h,t} + z^{RO}_{h,s,t} \Gamma^{RO} + p^{RO}_{h,s,t} \leqslant 0 \quad \forall h, \forall s, \forall t \tag{45}$$

$$z^{RO}_{h,s,t} + p^{RO}_{h,s,t} \geqslant P^{Wind\_Dev}_{h,s,t} y^{RO}_{h,s,t} \quad \forall h, \forall s, \forall t \tag{46}$$

$$-y^{RO}_{h,s,t} \leqslant x^{RO}_{h,s,t} \leqslant y^{RO}_{h,s,t} \quad \forall h, \forall s, \forall t \tag{47}$$

$$y^{RO}_{h,s,t}, p^{RO}_{h,s,t}, z^{RO}_{h,s,t} > 0 x^{RO}_{h,s,t} = 1 \quad \forall h, \forall s, \forall t \tag{48}$$

3.1.9. Electrical, thermal and natural gas equilibrium constraints

Electrical, thermal and natural gas consumption-production equilibrium is an essential part of the MES problem, which is indicated in equations Eqs. (49)-(51).

$$P^{EH}_{h,t} + P^{CHP}_{h,s,t} + P^{Wind}_{h,s.t} + P^{H2P}_{h,s,t} - P^{P2H}_{h,s,t} - P^{EB}_{h,s,t} - P^{D}_{h,s,t} = 0 \quad \forall h, \forall s, \forall t \tag{49}$$

$$H^{CHP}_{h,s,t} + H^{EB}_{h,s,t} + H^{ch}_{h,s,t} - H^{dis}_{h,s,t} - H^{D}_{h,s,t} = 0 \quad \forall h, \forall s, \forall t \tag{50}$$

$$G^{EH}_{h,s,t} + G^{dis}_{h,s,t} - G^{ch}_{h,s,t} - (\frac{P^{CHP}_{h,s,t}}{\eta^{CHP}_{h}} + SU_{h,s,t} + SD_{h,s,t}) - G^{D}_{h,s,t} = 0 \quad \forall h, \forall s, \forall t \tag{51}$$

3.2. Day-ahead wholesale market (Lower-level problem)

In the lower-level problem, WMO receives the offer/bids from producers/consumers and clears the DWM to maximize social welfare as it is derived in Eq. (52). In this equation, the first term represents the generation cost of GENCOs, while the second term is the cost of energy purchased/sold from/to MESs. The power flow equation of the TS is demonstrated in Eq. (53). Eqs. (54)-(55) impose the production limits of the GENCOs and power transfer limits of MES. The power transmission limits

as well as voltage angle bounds, are imposed by Eqs. (56)-(57), while Eq. (58) indicates the voltage angle in the slack bus.

$$\textbf{min} \left\{ \sum_{t} \sum_{g} C_{g}^{G} P_{g,t}^{G} - \sum_{t} \sum_{h} C_{h,t}^{EH} P_{h,t}^{ESP} \right\} \tag{52}$$

$$\sum_{g \in \mathcal{A}_i^g} P_{g,t}^{G} - \sum_{h \in \mathcal{A}_i^h} P_{h,t}^{EH} - P_{i,t}^{D} = \sum_{j \in Tr} B_{i,j}(\delta_{i,t} - \delta_{j,t}) : \lambda_{i,t}^{e} \;\; \forall b, \forall t \tag{53}$$

$$0 \leqslant P_{g,t}^{G} \leqslant P_{g,t}^{GMax} : \mu_{g,t}^{G\,min}, \mu_{g,t}^{G\,max} \;\; \forall g, \forall t \tag{54}$$

$$P_{h}^{EH,Min} \leqslant P_{h,t}^{EH} \leqslant P_{h}^{EH,Max} : \mu_{h,t}^{EH,min}, \mu_{h,t}^{EH,max} \;\; \forall t \tag{55}$$

$$-C_{i,j}^{Max} \leqslant B_{i,j}(\delta_{i,t} - \delta_{j,t}) \leqslant C_{i,j}^{Max} : \nu_{i,j,t}^{min}, \nu_{i,j,t}^{max} \;\; \forall i, \forall j, \forall t \tag{56}$$

$$-\pi \leqslant \delta_{i,t} \leqslant \pi : \xi_{i,t}^{min}, \xi_{i,t}^{max} \;\; \forall i, \forall t \tag{57}$$

$$\delta_{i=1,t} : \xi_{i=1,t}^{1} \;\; \forall i = 1, \forall t \tag{58}$$

3.3. The ultimate mathematical model

The proposed nonlinear bi-level optimization model is converted into a single-level MILP problem by KKT conditions using the strong duality theorem. The minutiae of this transformation are elaborated in Appendix B. Additionally, a thorough explanation is included in Appendix c to unravel the linearization method that is used to linearize the nonlinear term$\lambda_{i,t}^{e} P_{h,t}^{EH}$. Accordingly, the ultimate model is described as follows:

$$\textbf{min} \sum_{s} \pi_s \left\{ \sum_{t} \sum_{h} C_{h,t}^{g} G_{h,t,s}^{EH} + C_{h}^{P2H} P_{h,t,s}^{P2H} + (C_{h}^{dn} DR_{h,s,t}^{dn} + C_{h}^{up} DR_{h,s,t}^{up}) \right\} + X \tag{59}$$

subject to: Upper-level constraints: Equations. Eqs. (2)-(51). Lower-level constraints: Equations. Eq. (53) and Eqs. (b.2)-(b.13).

4. Numerical simulations

4.1. Data in brief

In this study, the lower-level problem (DWM) is modelled via two standard IEEE test systems. The IEEE 6-bus consists of 7 transmission lines, 2 load nodes and 3

GENCOs, while the IEEE 24-bus consists of 12 GENCOs, 14 load nodes and 37 transmission lines. The configuration and connection of the TS and MES (upper-level) are depicted in Figure 4. The parameters and data related to the TS, GENCO and transmission lines are available in [32, 47, 48], while the expected electric, heating and natural gas load profiles of the multi-energy system are shown in Figure 5, which are adopted from [49], and robust wind power profile is illustrated in [45]. Further, the MES is connected to TS through bus 5 (in IEEE 6-BUS) and 20 (in IEEE 24-bus) , and the crucial data related to the MES is summarized in Appendix C. The uncertainty of thermal, electrical and natural gas demand is modelled via stochastic programming with 1000 scenarios (created with normal distribution according to [50]), which are reduced down to the 10 most probable cases via SCENRED function in the GAMS environment, wherein scenario 8 is the worst-case scenario with highest thermal, natural gas and electricity demand. The proposed MILP is solved in GAMS environment by the standard CPLEX solver. To better evaluate the functionality of different components, the following case studies are designed.

- Case study 1 (**CS1**): An SP model to evaluate the strategic behavior of the MES in DWM without HES or DRP.
- Case study 2 (**CS2**): An SP model to evaluate the strategic behavior of the MES in DWM with HES.
- Case study 3 (**CS3**): An SP model to evaluate the strategic behavior of the MES in DWM with HES and DRP.
- Case study 4 (**CS4**): A hybrid RO-SP model to evaluate the strategic behavior of the MES in DWM with HES and DRP.

4.2. Results and discussions

CS1: The optimal scheduling of the MES for satisfying its electrical loads is illustrated in Figure 6. As can be seen, 28.05% of the demand is satisfied from DWM, 60.25% through CHP unit and 11.7% via wind turbines. Similarly, Figure 7 illustrates the way in which MES procures its thermal energy for thermal loads. It can be

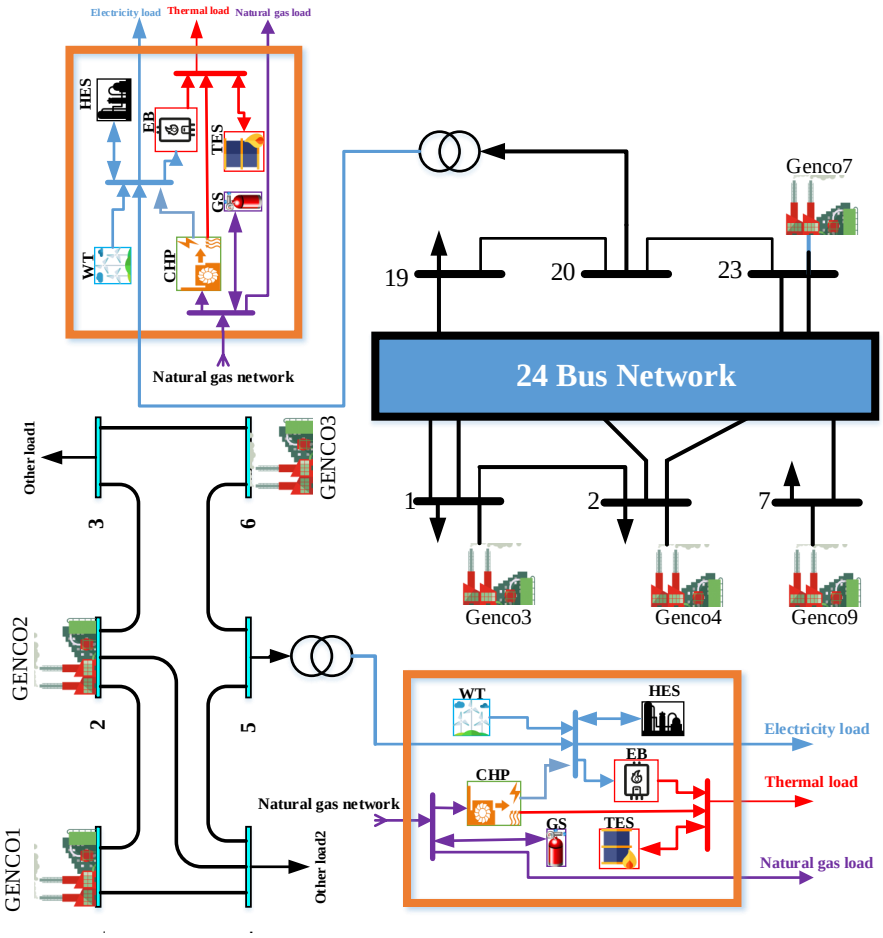

Figure 4: Overall structure of the MES in 6-bus and 24-bus TS

seen that 72.73% of the energy is satisfied by CHP unit, while 28.47% is supplied by EB. Moreover, the TES is charged during off-peak hours and discharged throughout the expensive peak hours, thereby enhancing the flexibility of the CHP unit. The hourly scheduling of GENCOs is depicted in Figure 8. It is readily apparent that GENCO1 (the cheapest and the largest GENCO) satisfies the largest portion of the load, which is equivalent to 4038.52 MWh. With the significant rise of the load demand in hours 8 and 12, GENCO2 and GENCO3 (slightly more expensive GENCOs) get into the system by generating 422.73 MWh and 307.97 MWh, respectively. The

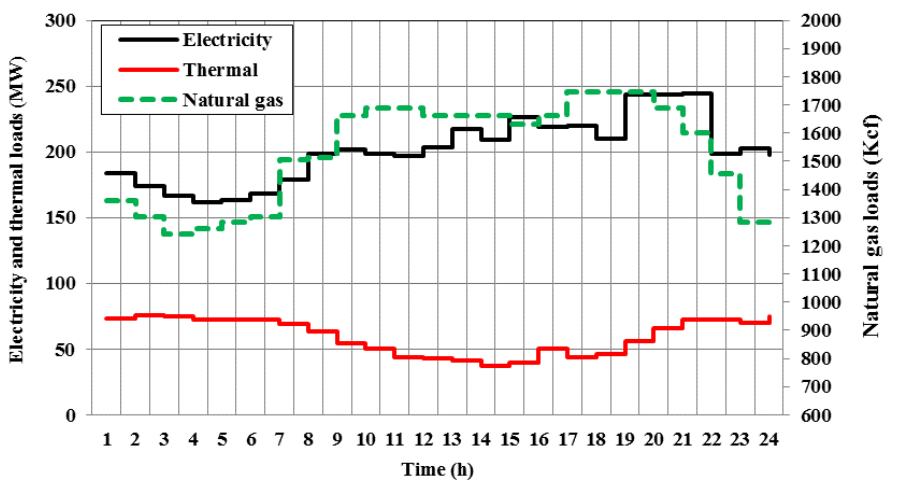

Figure 5: Electrical, thermal and natural gas loads of MES

line graph in Figure 8 illustrates the LMP. As can be observed, in the initial hours, insignificantly low demand can be satisfied by GENCO1 making the market-clearing price as low as 13.5 $/MWh. However, with increments in load demand, GENCO2 and GENCO3 inevitably enter the system, thereby leading to a steep surge in LMP (17.1 $/MWh at hour 8 and 26.25 $/MWh at 12). Nevertheless, extreme spikes in load demand, such as the incident at hour 21, can shoot up the price to 44.1 $/MWh.

CS2: The practical aspect of the HES is evaluated in this case. The optimal scheduling of MES is illustrated in Figure 9. According to the results, 20.11% of the electrical demand is satisfied through DWM, with 69.00% and 12.11% being supplied by CHP and wind turbines, respectively. As it can be inferred from Figure 10, the HES charges the hydrogen tanks during cheaper off-peak periods and then discharges it back to the MES in the form of electricity to support the system. The most prominent attribute of this storage capability is the notable reduction in LMP compared to that of the **CS1**. Figure 11 demonstrates the MES scheduling to satisfy thermal loads, which indicates that 95.43% of the thermal demand is accounted by CHP unit, whilst 4.55% of it is credited to EB. Figure 12 summarizes the optimal scheduling of the GENCOs in **CS2**. Based on the results, GENCO1 with 3923.63

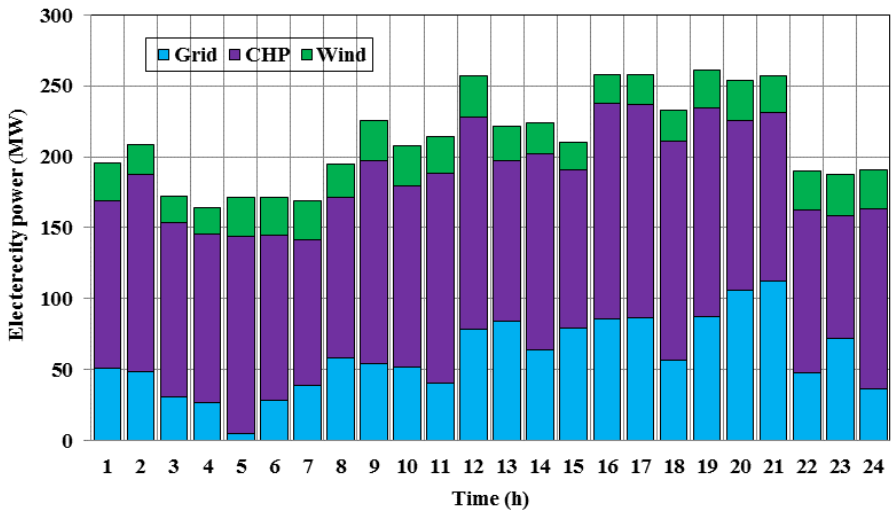

Figure 6: The optimal scheduling of MES to satisfy its demand in **CS1**

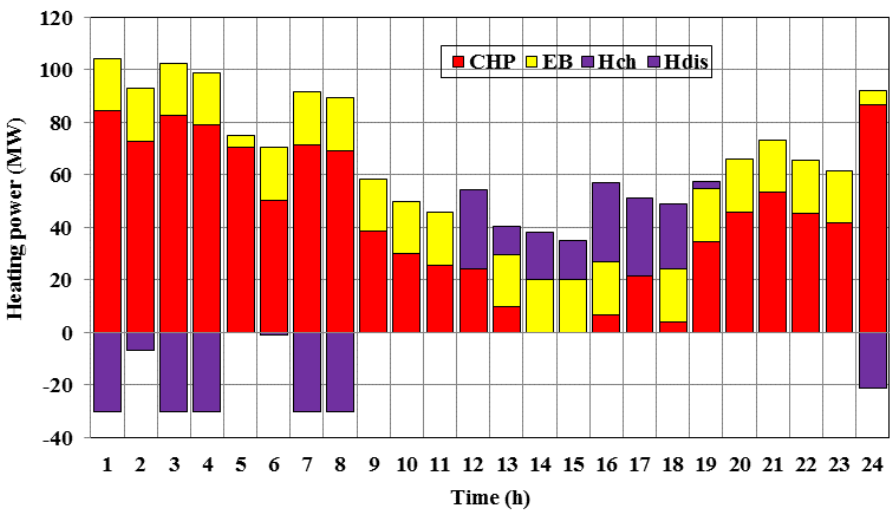

Figure 7: The optimal scheduling of MES to satisfy thermal demand in **CS1**

MWh production holds the largest share, which is followed by GENCO2 (201.27 MWh) and GENCO3 (204.96 MWh). Transparently, the usage of HES has influenced the production of the GENCOs in DWM. Most notably, in comparison with **CS1**, the production of GENCO1, GENCO2 and GENCO3 has respectively plunged by 114.89 MWh, 221.46 MWh and 103.01 MWh. Figure 13 provides a comparative

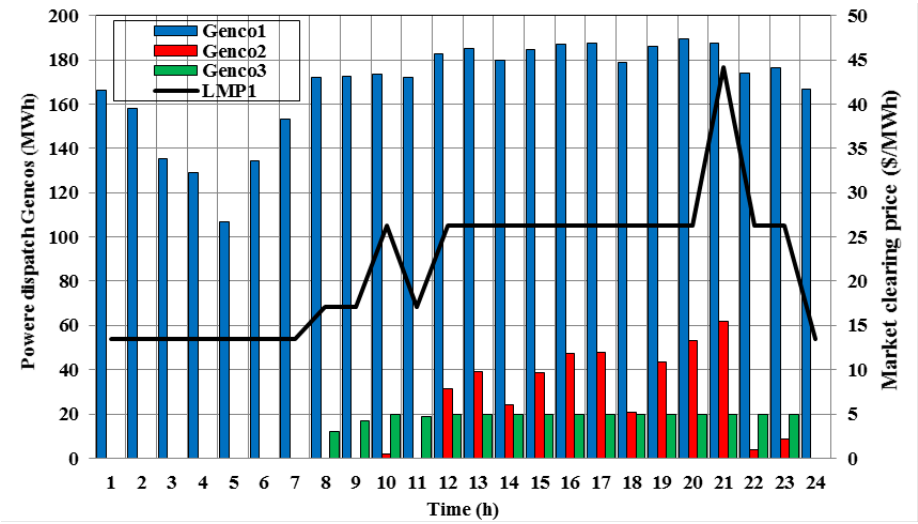

Figure 8: Optimal scheduling of GENCOs and LMP in **CS1**

look into the LMP of **CS1** and **CS2**. According to the obtained values, GENCO1 is the only responsive unit from hours 1 to 11, which leads to the LMP value of 13.5 $/MWh. Nonetheless, with the rapid rise in load demand at hour 12, GENCO2 (as a relatively expensive unit) gets into the system, thereby increasing the LMP up to 26.25 $/MWh. It is noteworthy that the inclusion of HES brings down the LMP by 72.45 $/MWh.

CS3: Apart from HES, this case also includes DRP in the problem. It should not be left unmentioned that DRP is only applied to the electrical loads. Therefore, this case only focuses on the electrical side of the problem. The optimal scheduling of MES to satisfy electrical loads is illustrated in Figure 14. Based on the obtained results, 96.33% of demand is satisfied through DWM, while CHP unit and wind turbines respond to 19.54% and 12.19% of it respectively. Moreover, it can be construed that DRP shifts 10% of the load from peak periods to off-peak hours. Consequently, the amount of energy that is procured from DWM in peak hours, shifts back to the time periods wherein most GENCOs are idle and LMP is low. In other words, compared to **CS2**, DRP improves the flexibility of the MES in exploiting cheaper market periods. Figure 15 demonstrates optimal hourly scheduling of

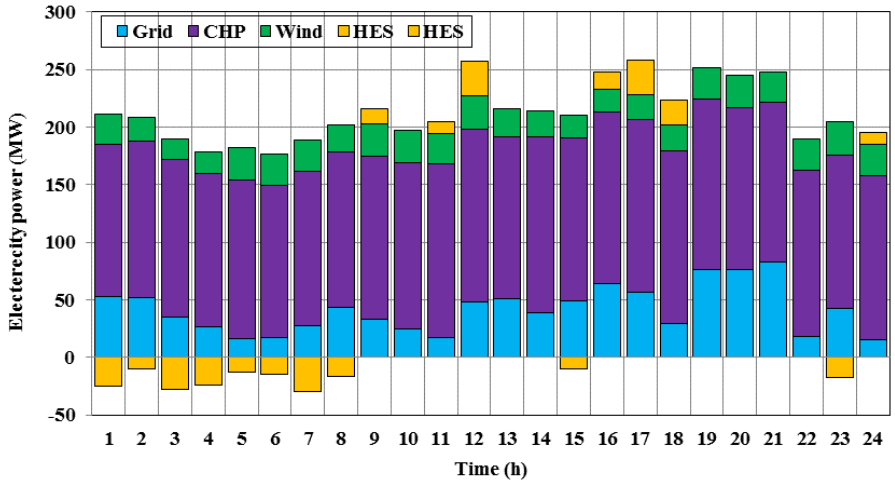

Figure 9: Optimal scheduling of the MES for satisfying load demand in **CS2**.

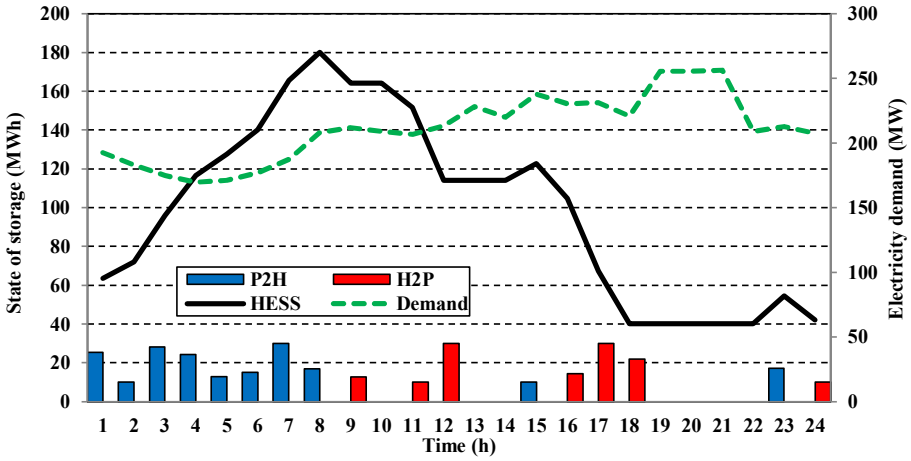

Figure 10: The way of storing energy in HES vs load demand in **CS2**

GENCOs in **CS3**. In reference to obtained values, GENCO1, GENCO2 and GENCO3 account for 4032.6 MWh, 42.42 MWh and 220 MWh, respectively. Most significantly, in comparison to **CS2**, due to the fact that a higher portion of the energy is procured during off-peak hours, the production of GENCO1 and GENCO3 has surged by 108.97 MWh and 15.03 MWh, respectively. In contrast, the production of the GENCO2 has plummeted by 158.84 MWh since it is the most expensive unit.

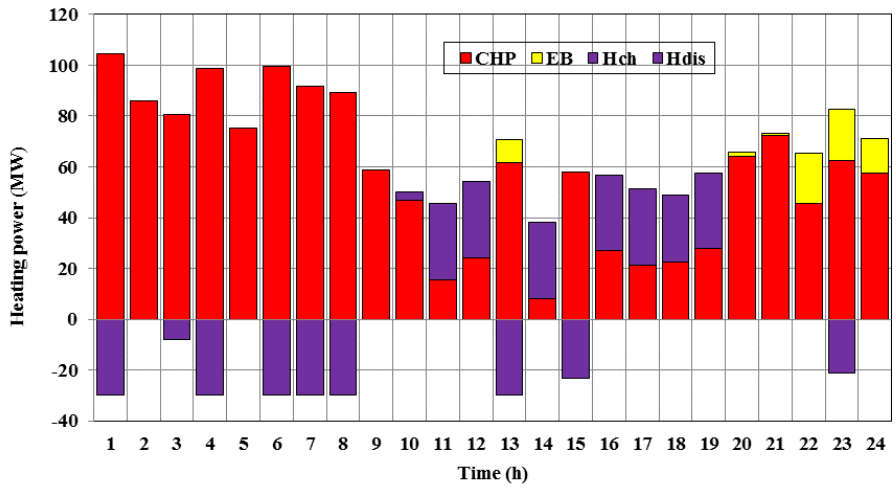

Figure 11: Optimal scheduling of the MES for satisfying thermal demand in **CS2**

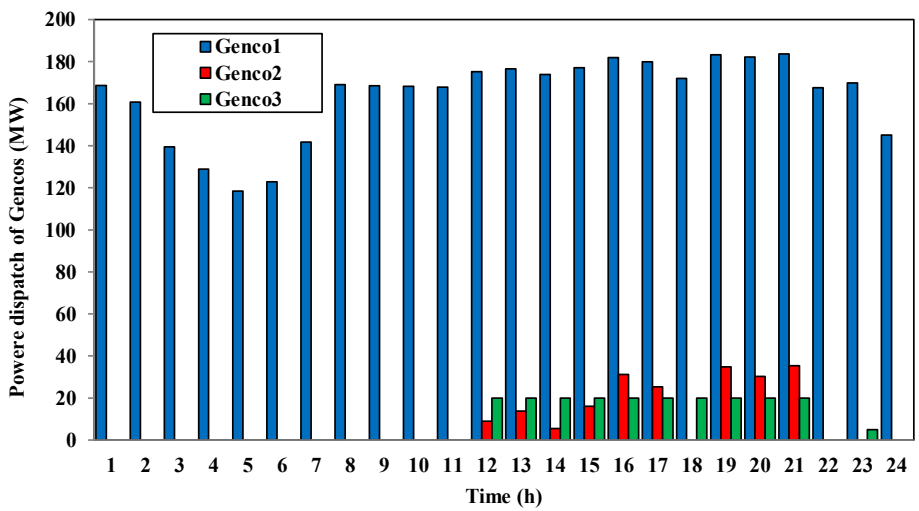

Figure 12: Optimal scheduling of each GENCO in **CS2**

The LMP of **CS3** is compared to the results of **CS2** and **CS3** in Figure 16. As can be observed, integrating DRP in **CS3** leads to 23.13 $/MWh (compared to **CS2**) and 109.08 $/MWh (compared to **CS1**) decline in the LMP. Moreover, two sensitivity analysis has been introduced in this case to better evaluate the efficacy of the DRP. Figure 17 illustrates the impacts of increasing load-shifting factor of DRP. It can

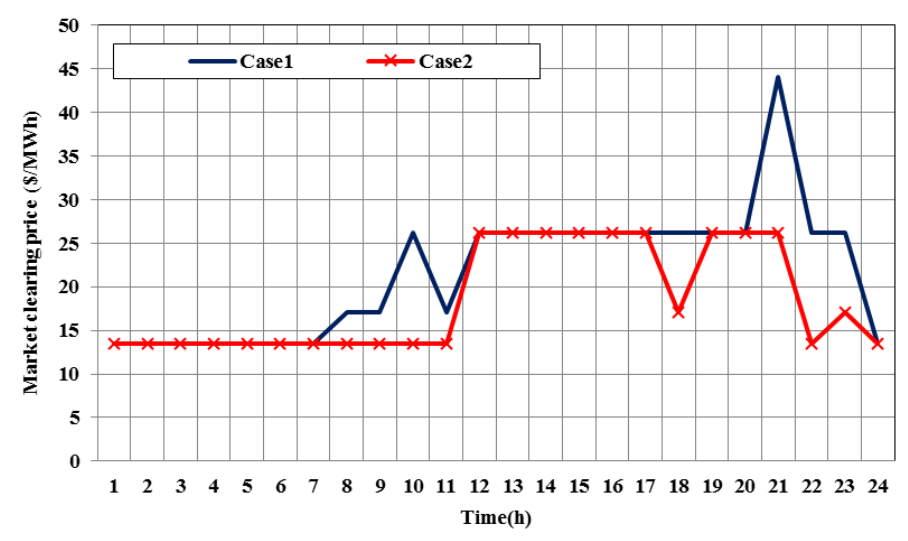

Figure 13: Comparison of the LMP in **CS1** and **CS2**

be noted that increasing this shifting coefficient enhances the elasticity of the MES in shifting demand to cheaper off-peak operation regions. Furthermore, Figure 18 demonstrates the impacts of increasing shifting-factor on LMP. It is observed that the load factor in inversely proportional to the LMP.

CS4: This case is designed to evaluate the proposed hybrid RO-SP approach in dealing with uncertainty behavior of the strategic DWM, which schedules MES with HES and DRP. In this case, the intermittent nature of wind power is modelled via robust optimization approach and sensitivity of the problem for robustness spectrum of $\Gamma = 0$ to $\Gamma = 1$ is evaluated. In $\Gamma = 0$ the uncertainty of wind power is ignored, while when $\Gamma = 1$, the problem provides the most reliable and conservative solutions regarding the arbitrary nature of the wind power. To illustrate the impact of uncertainty on LMP, the uncertainty quota (Γ) is given values in the interval of (0,1) with step width of 0.2. The results of the sensitivity analysis on wind power and LMP is illustrated by Figure 19 and Figure 20, respectively. As can be observed, increasing the value Γ, leads to lower wind power production. The reason is that the MES operator prefers to take lower risks in regards to wind power production, and that comes with conservatism in solutions. Consequently, the MES operator is

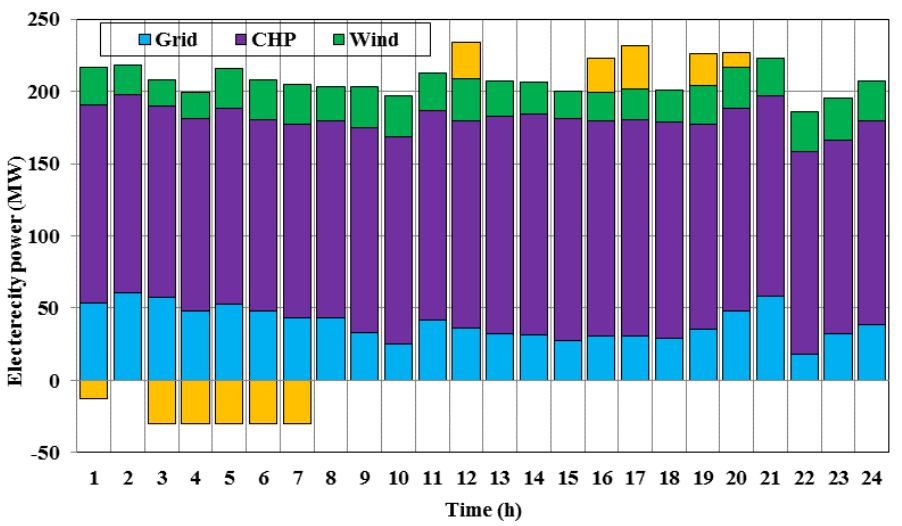

Figure 14: The hourly scheduling of the MES to satisfy electrical demand in **CS3**

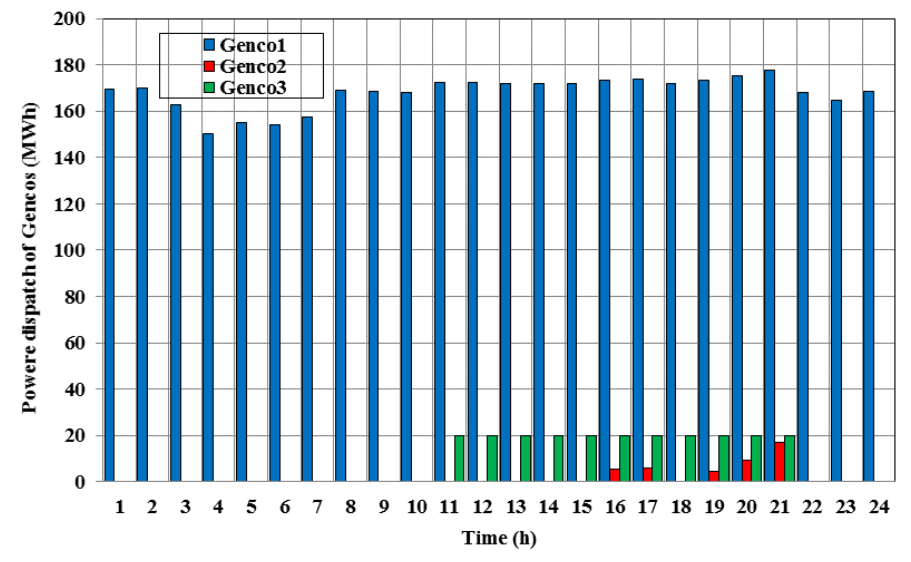

Figure 15: The hourly scheduling of the GENCOS in **CS3**

obliged to import a higher share of its demand through DWM, Which leads to inclusion of the expensive GENCOs that increase the overall LMP. Based on the results of Figure 20, the conservative RO-SP (when $\Gamma = 1$) can lead to 3.12% higher LMP

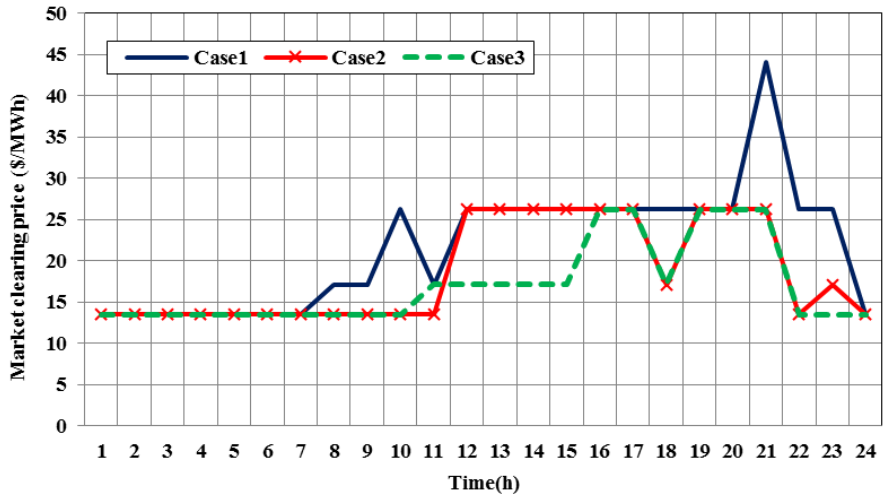

Figure 16: Comparison of LMP price in **CS3** and other Cases

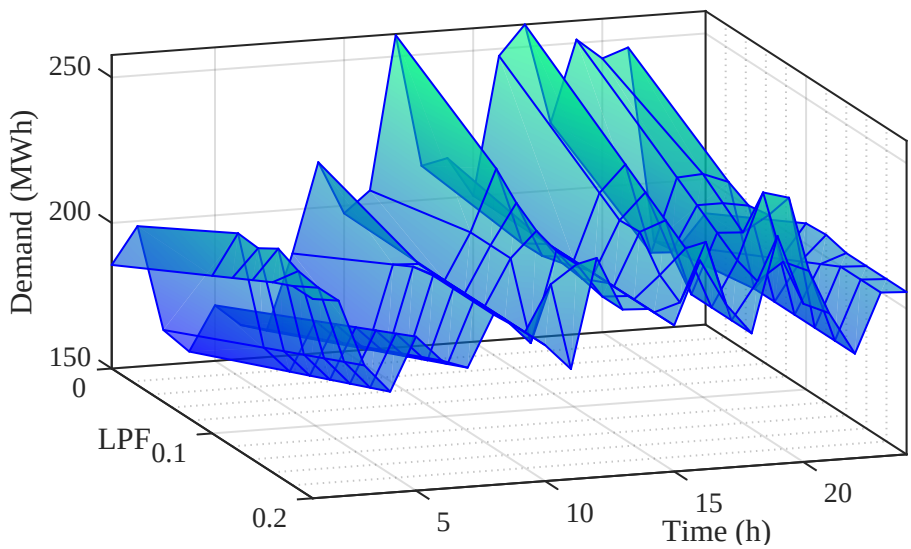

Figure 17: Sensitivity analysis on load-shifting factor on the demand profile of the MES

in regard to deterministic scheme (when $\Gamma = 0$). Furthermore, the sensitivity analysis of (Γ) on total operational cost of the MES operator is included in Figure 21. Accordingly, the previous hypothesis are still valid and higher values of (Γ) leads to increments in cost, which is the the value that is paid more conservative footsteps.

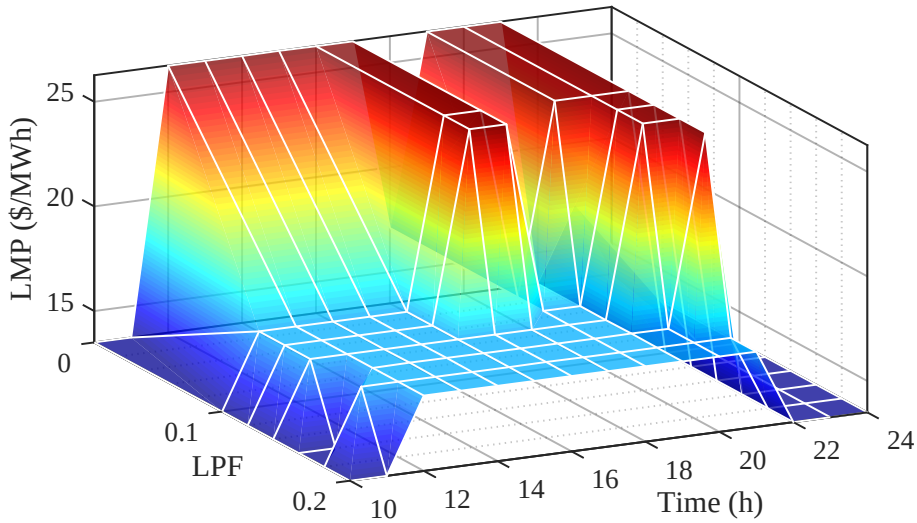

Figure 18: Sensitivity analysis of the load-shifting factor on LMP in **CS3**.

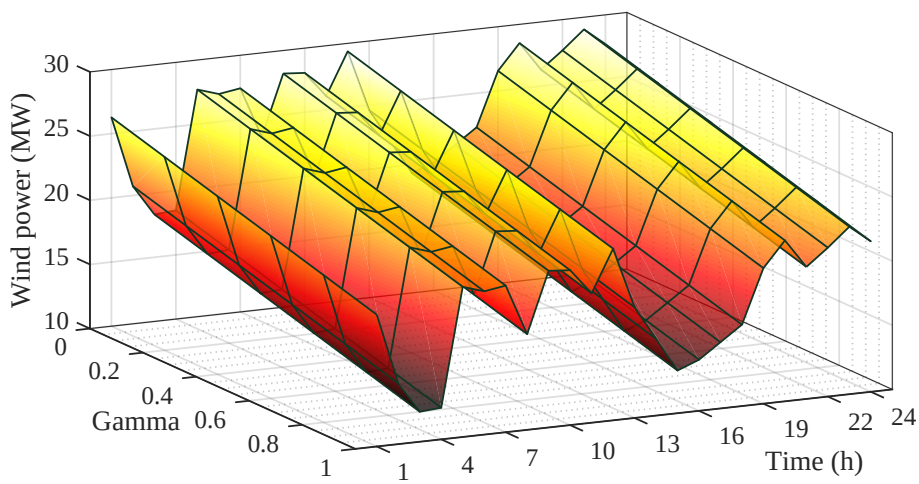

Figure 19: Wind power production for different robustness schedules in **CS4**

4.3. Comparative evaluations

The total expected cost value in all 4 cases of the MES is summarized in Table 1. Based on these findings, the following facts can be inferred.

1. Utilizing HES in **CS2** of MES brings down the total operation cost by 5.35% in the worst case scenario (8th stochastic scenario) and by 5.46% in expected

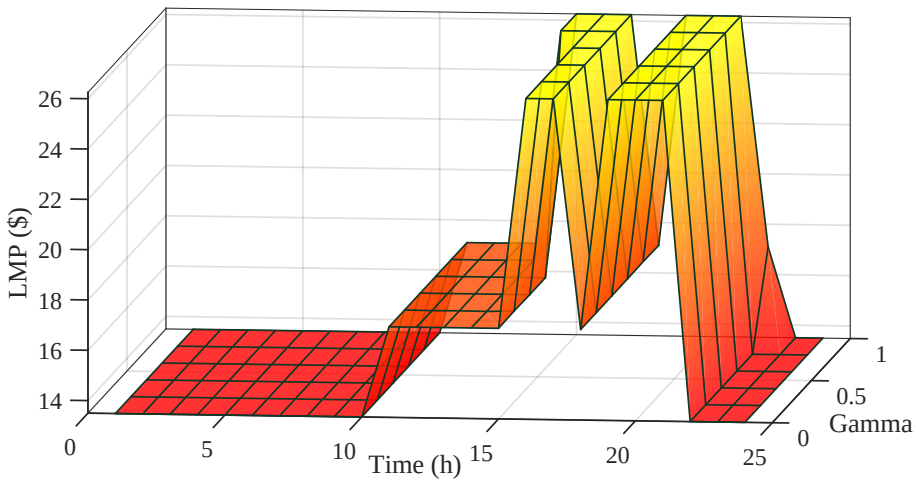

Figure 20: The LMP for different robustness schedules in **CS4**

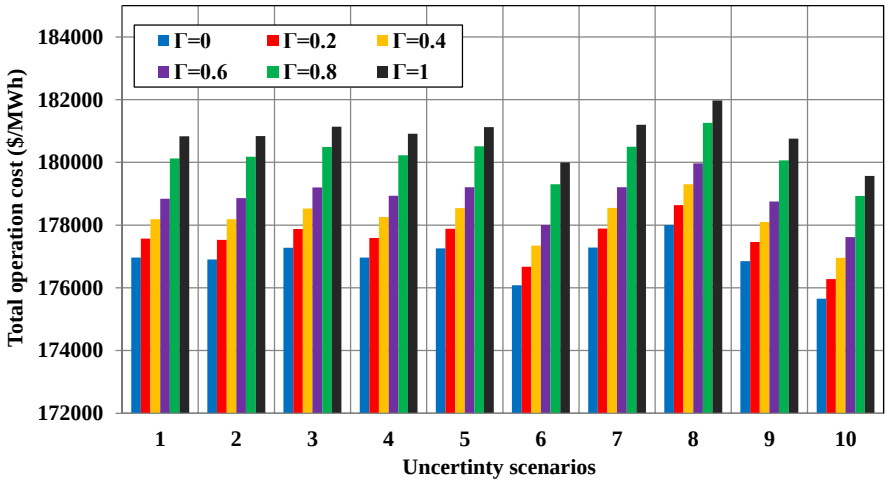

Figure 21: Total operational cost in various scenarios regarding different robustness values

value when compared to **CS1**.

2. In comparison to **CS1**, incorporating DRP in **CS3** reduces the operation cost of scenario 8 (the worst scenario) by 8.36% and the expected value by 8.14%.
3. Incorporating hybrid RO-SP in **CS4**, turns this case into the most conservative and robust case study. As can be seen, the cost values of the worst-case sce-

nario (scenario 8) and the expecte 2.17% and 2.15%, respectively ,compared to **CS3**.

Table 2 summarizes total operational costs of MES in 4 cases and 10 distinct stochastic scenarios. As can be seen, scenario 10 is the most optimistic scenario, while scenario 8 carries the most pessimistic outcome.

Table 1: The Operational cost comparison in different cases

	CS1 ($/MWh)	CS2 ($/MWh)	CS3 ($/MWh)	CS4 ($/MWh)
Power purchased in DWM	41130.04	26015.73	19825.62	23793.31
Gas purchased	152661.2	157171.6	157392.3	157402.12
HES costs	0	265.1765	227.2941	210.00
DRP costs	0	0	563.39	567.69
Total operation costs in scenario 8	193791	183452.5	178008.6	181973.10
Expected Gas purchased	151958	156314.3	156509.8	156504.89
Expected operation costs	193088	182535.6	176944.1	180850.21

4.4. IEEE 24-bus test system

For further verification of the outcomes, all case studies of MES are also evaluated on this bigger 24-bus test system. The LMP of the DWM in three cases is demonstrated by Figure 22. According to the empirical outcomes, incorporating HES can diminish LMP as much as 1.67% in **CS2** compared to **CS1**. In other word, the MES operator is a price-maker in hours 13 and 17. Moreover, when MES is equipped with DRP in **CS3**, the LMP plummets by 3.13%, and it can be construed that MES turns into a price-maker in hours 14,17 and 20. The variations on the amount of energy that is purchased by MES throughout different cases can be observed in Figure 23. As can be seen, when the HES (**CS2**) and DRP (**CS3**) are integrated in MES, the energy import falls by 1.35% and 2.04%, respectively. However, when the hybrid RO-SP approach is deployed in **CS4** the total cost rises by 1.09% in regard to **CS3**. Furthermore, a sensitivity analysis is conducted on robust-

Table 2: Total operational costs in 4 cases and 10 scenarios

Scenario	Probability	CS1 ($/MWh)	CS2 ($/MWh)	CS3 ($/MWh)	CS4 ($/MWh)
1	0.0293	192948.7	182463.1	176966.8	180128
2	0.0725	193225.5	182556.5	176907.2	180176.6
3	0.1819	193265.3	182884.3	177278.9	180494.5
4	0.0687	193244.2	182574.4	176965.1	180225.8
5	0.1095	192987.8	182848.4	177259.8	180510.9
6	0.0795	192219.4	181752.1	176082.7	179304.3
7	0.0314	193503.2	182929.2	177284	180501
8	0.14	193791.2	183452.5	178008.6	181259.8
9	0.1539	193432	182399.4	176852.2	180064.8
10	0.1333	192088.4	181356	175653.8	178930.3

ness adjustment parameter of the RO in Figure 24. As can be seen, increasing the robustness comes with higher cost, while making the MES more robust regarding wind power uncertainty. Eventually, the overall costs of IEEE 24-bus systems are summarized in Table 3.

Table 3: Total operational costs in 4 cases and 10 scenarios

	CS1	CS2	CS3	CS4
Energy purchased in DWM ($/MWH)	20574.99	13842.63	11833.73	13701.05
Purchased natural gas ($/MWH)	152608.4	156971.9	157337.8	157337.85
HESS costs ($/MWH)	0	232.7753	141.1334	141.13
DRP costs ($/MWH)	0	0	636.0383	636.04
Total operation costs in scenario 8 ($/MWH)	173183.4	171047.3	169948.7	171816.06
Expected gas purchase ($/MWH)	151891.1	156114.3	156555.3	156555.32
Expected operational cost ($/MWH)	172466.1	170140.2	168947.3	170814.63

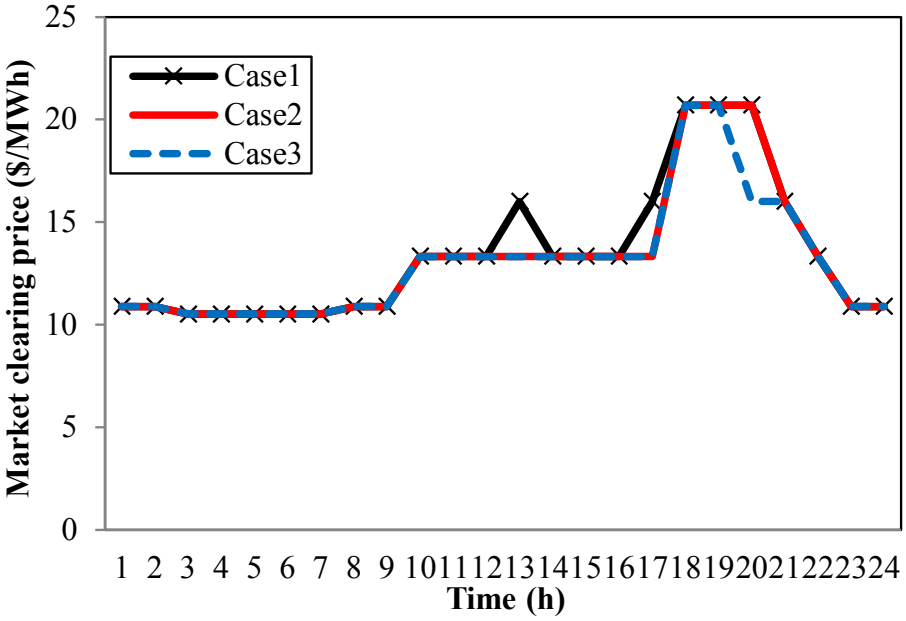

Figure 22: The LMP of different cases in IEEE 24-bus

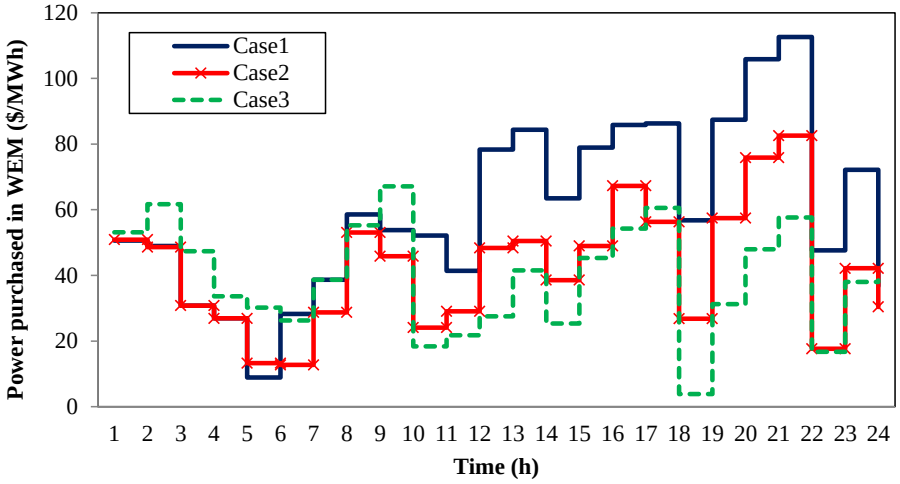

Figure 23: The power MES purchased from DWM in IEEE 24-bus

5. Conclusion

This study investigated the strategic scheduling of MES as a price-setter in DWM with flexible DRP and HES technologies. In this regard, an unique bi-level optimiza-

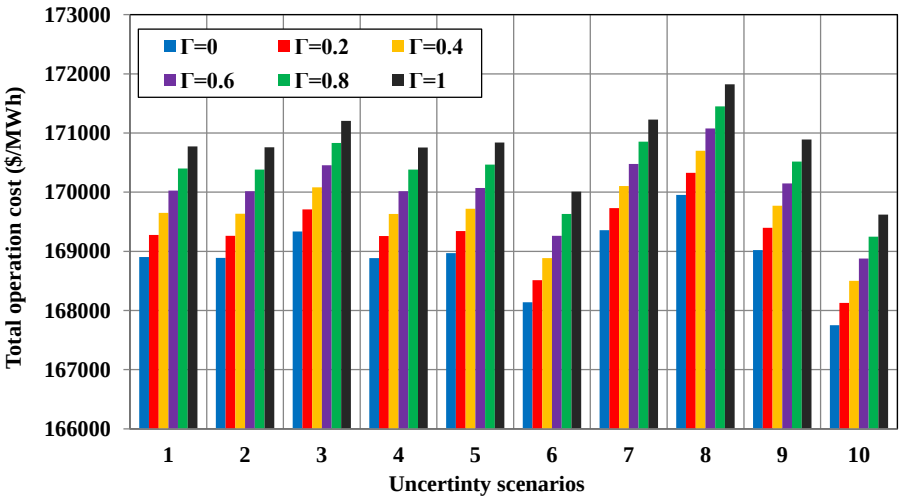

Figure 24: The sensitivity analysis on robustness in IEEE 24-bus

tion framework was deployed, wherein the upper-level problem is a hybrid RO-SP-based MES that has the objective of minimizing operational costs and the cost of procuring energy from DWM, while the lower-level problem is the WMO that clears DWM to maximize public satisfaction. The obtained nonlinear bi-level problem was converted into a single-level MILP problem through KKT conditions and the theory of strong duality. Moreover, the uncertain nature of the wind power was handled by a RO model, while other uncertain parameters were defined as finite stochastic scenarios. The results were verified on IEEE 6-bus and more realistic IEEE 24-bus TS. The most noteworthy findings of this study can be summarized as follows:

- The participation of MES as a price-maker player in DWM leads to a notable amount of decline in LMP.
- The Incorporation of flexible energy technologies, such as HES and DRP, alters the strategic behavior of the MES in DWM. In this concern, the results of the cases with HES and DRP are self-explanatory.
- Increasing the load-shifting factor of DRP boosts the elasticity of the MES in shifting load demand to cheaper off-peak hours.

- Increasing the robustness of the system against wind power uncertainty in RO-SP method leads to a higher amount of cost since the wind power is scheduled under more conservative speculations and that results in higher LMP. Nevertheless, higher robustness improves the reliability of the system.

Appendix A. Hybridized robust optimization and stochastic programming (RO-SP) method

A conventional SP problem is defined as follows [51]:

$$\min \sum_{s} \pi_s \sum_{j \in WS} c'_{s,j} x_{s,j} + \sum_{j \in HN} c_j x_j \tag{a.1}$$

$$\sum_{j \in WS} A'_{s,j,i} x_{s,j} + \sum_{j \in HN} A_{j,i} x_j \leqslant b_{s,i}, \sum_{j \in WS} A'_{s,j,i} x_{s,j} + \sum_{j \in HN} A_{j,i} x_j = g_{s,i} \tag{a.2}$$

Wherein, s: index of SP scenario, j: index of variables, i: index of constraints, WS: set of wait and see variables, HN: set of here and now variables, π_s: the occurrence probability of scenarios, $c'_{s,j}$: set of uncertain parameters in the objective function, c_j: set of known parameters in the objective function, $A'_{s,j,i}$: set of uncertain parameters in the constraints, $A_{j,i}$: set of known parameters in the constraints. $b_{s,i}/g_{s,i}$: the uncertain parameters in inequality and equality constraints.

As illustrated, in a generic SP problem, there are two types of variables that are classified as here-and-now (decision that are made now) and wait-and-see variables (decisions that depend on the outcomes of the SP scenarios). The problem with SP method is that it only minimizes the expected value of objective, which might provide some very high-cost and risky solutions. Moreover, some real-world parameters are very erratic and do not follow any probability distributions to generate SP scenarios. On the other hand, the RO method is very suitable for variables that do not possess a probability distribution. Although RO is a risk-averse uncertainty method, it can provide very conservative solutions that is not necessary for some uncertain parameters. In the light of these facts, this paper has utilized a hybrid RO-SP method. The erratic and high risk parameters (i.e., wind power production) are modelled by RO method that does not require probability distributions, and the parameters that have detectible probability distribution and follow specific

distributions (i.e., thermal, electrical and natural gas demand) are modelled as SP scenarios. The overall mathematical formulation of the RO-SP is established as follows:

$$\min \sum_{s} \pi_s \left(\sum_{j \in WS} c'_{s,j} x_{s,j} + \sum_{j \in HN} c_j x_j + z_0 \Gamma_0 + \sum_{j=J_0} \phi_{s,0,j} \right) \tag{a.3}$$

$$z_0 + \phi_{s,0,j} \geqslant D_j \Upsilon_{s,j} \forall s, j \in J_0 \tag{a.4}$$

$$z_i + \phi_{s,j,i} \geqslant \hat{A}_{j,i} \Upsilon_{s.i} \forall s, j \in J_i, i \neq 0 \tag{a.5}$$

$$-\Upsilon_{s,j} \leqslant x_{s,j} \leqslant \Upsilon_{s,j} \forall s, j \tag{a.6}$$

$$L_j \leqslant x_{s,j} \leqslant U_j \forall s, j \tag{a.7}$$

$$\phi_{s,j} \geqslant 0, \Upsilon_{s,j} \geqslant 0, z_{s,i} \geqslant 0 \forall s, i \tag{a.8}$$

Wherein, $z_0/\phi_{s,0,j}/z_i/\phi_{s,j,i}/\Upsilon_{s,j}$: auxiliary variables defined in robust optimization to obtain a mixed-integer robust formulation, Γ_0/Γ_i: Robustness controller in the objective function and the constraints, respectively. $D_j/\hat{A}_{j,i}$: forecasted deviation of the parameters from expected value in objective function and constraints. L_j/U_j: the upper and lower bounds of the variables. The above-mentioned model on RO is proven from theory of strong duality in [46].

Appendix B. Mathematical program with equilibrium constraints (MPEC)

KKT conditions are one of the most effective ways of converting linear convex optimization problems into a single-level one. In the current study, the lower-level problem (social welfare maximization by WMO) is a linear and convex model, which can be replaced by its KKT conditions as they are categorized in the following four conditions:

Appendix B.0.1. Stationary constraints

First, the Lagrange function of the lower-level problem should be obtained as illustrated in Eq. (b.1), wherein $f(x)$ $h(x)$ and $g(x)$ and are the objective, equality and inequality functions, while x is denoted as decision variable vector. Eventually,

the stationary constraints are evaluated from derivatives of the Lagrange function over every single decision variable.

$$L = f(x) + \lambda^T h(x) + \mu^T g(x) \tag{b.1}$$

$$\frac{\partial L}{\partial P^G_{g,t}} = C^G_g - \lambda^e_{i,t} + \mu^{G\,max}_{g,t} - \mu^{G\,min}_{g,t} = 0 \;\; \forall g \in A^g_i, \forall i, \forall t \tag{b.2}$$

$$\frac{\partial L}{\partial P^{EH}_{h,t}} = -C^{EH}_{h,t} + \lambda^e_{i,t} + \mu^{EH,max}_{h,t} - \mu^{EH,min}_{h,t} = 0 \;\; \forall h \in A^h_i, \forall i, \forall t \tag{b.3}$$

$$\begin{aligned} \tfrac{\partial L}{\partial \delta_{j,t}} = & \sum_{j \in Tr} B_{i,j}(\lambda^e_{i,t} - \lambda^e_{i,t}) + \sum_{j \in Tr} B_{i,j}(\nu^{max}_{i,j,t} - \nu^{max}_{j,i,t}) \\ & + \sum_{j \in Tr} B_{i,j}(\nu^{min}_{j,i,t} - \nu^{min}_{i,j,t}) + \xi^{max}_{i,t} - \xi^{min}_{i,t} + \xi^1_{i=1,t} = 0 \end{aligned} \quad \forall i, \forall t \tag{b.4}$$

Appendix B.0.2. Primal, dual, and complementary constraints

$$0 \leqslant P^G_{g,t} \perp \mu^{G\,min}_{g,t} \geqslant 0 \;\; \forall g, \forall t \tag{b.5}$$

$$0 \leqslant (P^{EH}_{h,t} - P^{EH,min}_{h,t}) \perp \mu^{EH,min}_{h,t} \geqslant 0 \;\; \forall h, \forall t \tag{b.6}$$

$$0 \leqslant (P^{G\,max}_{g,t} - P^G_{g,t}) \perp \mu^{G\,max}_{g,t} \geqslant 0 \;\; \forall g, \forall t \tag{b.7}$$

$$0 \leqslant (P^{EH,max}_h - P^{EH}_{h,t}) \perp \mu^{EH,max}_{h,t} \geqslant 0 \;\; \forall h, \forall t \tag{b.8}$$

$$0 \leqslant (C^{Max}_{i,j} + B_{i,j}(\delta_{i,t} - \delta_{j,t})) \perp \nu^{min}_{i,j,t} \geqslant 0 \;\; \forall i, \forall j, \forall t \tag{b.9}$$

$$0 \leqslant (C^{Max}_{i,j} - B_{i,j}(\delta_{i,t} - \delta_{j,t})) \perp \nu^{max}_{i,j,t} \geqslant 0 \;\; \forall i, \forall j, \forall t \tag{b.10}$$

$$0 \leqslant (\pi - \delta_{i,t}) \perp \xi^{max}_{i,t} \geqslant 0 \;\; \forall i, \forall t \tag{b.11}$$

$$0 \leqslant (\pi + \delta_{i,t}) \perp \xi^{min}_{i,t} \geqslant 0 \;\; \forall i, \forall t \tag{b.12}$$

To linearize the nonlinear term in Eqs. (b.5)-(b.12), the following procedure is followed. Here, M_1 and M_2 are large constants, while u is a binary variable.

$$\begin{aligned} & 0 \leqslant g_x \perp \mu \geqslant 0 \rightarrow g_x \geqslant 0, \mu \geqslant 0 \\ & g_x \leqslant M_1 u, \mu \leqslant M_2(1-u) \end{aligned} \tag{b.13}$$

Appendix C. Linearization of . $\lambda^{e}_{i,t}P^{EH}_{h,t}$

As observed from Eq. (1), the term $\lambda^{e}_{i,t}P^{EH}_{h,t}$ is a nonlinear expression. In this concern, the strong duality theorem is deployed to find a linear equivalent. The framework can be mathematically expressed as follows:

$$\mathrm{Max}\sum_{t}\left[\begin{array}{l} -\sum_{g}P^{GMax}_{g,t}\mu^{GMax}_{g,t}+\sum_{h}P^{EH,Min}_{h,t}\mu^{EH,Min}_{h,t}-\sum_{h}P^{EH,Max}_{h,t}\mu^{EH,Max}_{h,t} \\ -\sum_{i,j\in Tr}\nu^{min}_{i,j,t}C^{max}_{i,j,t}-\sum_{i,j\in Tr}\nu^{max}_{i,j,t}C^{max}_{i,j,t}-\sum_{i}\pi(\xi^{max}_{i,t}+\xi^{min}_{i,t})+\sum_{i}P^{D}_{i,t}\lambda^{e}_{i,t} \end{array}\right] \tag{c.1}$$

According to strong duality, primal and dual objectives can be equalized:

$$\begin{aligned} &\sum_{t}\left[\begin{array}{l} -\sum_{g}P^{GMax}_{g,t}\mu^{GMax}_{g,t}+\sum_{h}P^{EH,Min}_{h,t}\mu^{EH,Min}_{h,t}-\sum_{h}P^{EH,Max}_{h,t}\mu^{EH,Max}_{h,t} \\ -\sum_{i,j\in Tr}\nu^{min}_{i,j,t}C^{max}_{i,j,t}-\sum_{i,j\in Tr}\nu^{max}_{i,j,t}C^{max}_{i,j,t}-\sum_{i}\pi(\xi^{max}_{i,t}+\xi^{min}_{i,t})+\sum_{i}P^{D}_{i,t}\lambda^{e}_{i,t} \end{array}\right] \\ &=\sum_{g}\sum_{t}C^{G}_{g}P^{G}_{g,t}-\sum_{t}\sum_{h}C^{EH}_{h,t}P^{EH}_{h,t} \end{aligned} \tag{c.2}$$

To obtain the nonlinear term $\lambda^{e}_{i,t}P^{EH}_{h,t}$, Eq. (b.3) is multiplied by $P^{EH}_{h,t}$ as follows:

$$\begin{aligned} &-P^{EH}_{h,t}C^{EH}_{h,t}+P^{EH}_{h,t}\lambda^{e}_{i,t}+P^{EH}_{h,t}\mu^{EH,max}_{h,t}-P^{EH}_{h,t}\mu^{EH,min}_{h,t}=0 \\ &0\leqslant(P^{EH}_{h,t}-P^{EH,min}_{t})\perp\mu^{EH,min}_{h,t}\geqslant 0\rightarrow P^{EH}_{h,t}\mu^{EH,min}_{h,t}=P^{EH,min}_{h,t}\mu^{EH,min}_{h,t} \\ &0\leqslant(P^{EH,max}_{h}-P^{EH}_{h,t})\perp\mu^{EH,max}_{h,t}\geqslant 0\rightarrow P^{EH}_{h,t}\mu^{EH,max}_{h,t}=P^{EH,max}_{h,t}\mu^{EH,max}_{h,t} \\ &P^{EH}_{h,t}C^{EH}_{h,t}=P^{EH}_{h,t}\lambda^{e}_{i,t}+P^{EH,max}_{h,t}\mu^{EH,max}_{h,t}-P^{EH,min}_{h,t}\mu^{EH,min}_{h,t} \end{aligned} \tag{c.3}$$

$$\sum_{t}\sum_{h}P^{EH}_{h,t}C^{EH}_{h,t}=\sum_{t}\sum_{h}P^{EH}_{h,t}\lambda^{e}_{i,t}+\sum_{t}\sum_{h}P^{EH,max}_{h}\mu^{EH,max}_{h,t}-\sum_{t}\sum_{h}P^{EH,min}_{h}\mu^{EH,min}_{h,t} \tag{c.4}$$

Eventually, the term $\lambda^{e}_{i,t}P^{EH}_{h,t}$ is substituted as follows:

$$\begin{aligned} &\sum_{t}\sum_{h}C^{EH}_{h,t}P^{EH}_{h,t}=\sum_{g}\sum_{t}C^{G}_{g}P^{G}_{g,t} \\ &-\sum_{t}\left[\begin{array}{l} -\sum_{g,b}P^{GMax}_{g,t}\mu^{GMax}_{g,t}+\sum_{h,t}P^{EH,Min}_{h,t}\mu^{EH,Min}_{h,t}-\sum_{h,t}P^{EH,Max}_{h,t}\mu^{EH,Max}_{h,t} \\ -\sum_{i,j\in Tr}\nu^{min}_{i,j,t}C^{max}_{i,j,t}-\sum_{i,j\in Tr}\nu^{max}_{i,j,t}C^{max}_{i,j,t}-\sum_{i}\pi(\xi^{max}_{i,t}+\xi^{min}_{i,t})+\sum_{i}P^{D}_{i,t}\lambda^{e}_{i,t} \end{array}\right] \end{aligned} \tag{c.5}$$

$$
\begin{aligned}
X = & \sum_{h}\sum_{t} P^{EH}_{h,t}\lambda^{e}_{b,t} = \sum_{g}\sum_{t} C^{G}_{g} P^{G}_{g,t} \\
& -\sum_{t}\left[\begin{array}{l} -\sum_{g,b} P^{GMax}_{g,t}\mu^{GMax}_{g,t} - \sum_{b,b'\in\theta_b} \nu^{min}_{b,b',t} C^{max}_{b,b',t} - \sum_{i,j\in Tr} \nu^{min}_{i,j,t} C^{max}_{i,j,t} \\ -\sum_{i,j\in Tr} \nu^{max}_{i,j,t} C^{max}_{i,j,t} - \sum_{i} \pi(\xi^{max}_{i,t} + \xi^{min}_{i,t}) + \sum_{i} P^{D}_{i,t}\lambda^{e}_{i,t} \end{array}\right]
\end{aligned} \tag{c.6}
$$

Appendix D. Multi-energy system (MES) parameters and data

Table D.4: Problem parameters

Equipment	Parameter	Amount	Equipment	Parameter	Amount
CHP unit	P^{Min}_{h}	46MW	HES	A^{Min}_{h}/A^{Max}_{h}	40MW / 180MW
	P^{Max}_{h}	155MW		$A^{HES}_{h,s,t=1}/A^{HES}_{h,s,t=24}$	42MW
	R^{up}_{h}/R^{dn}_{h}	40MW/40MW		$P^{P2H}_{h,Max}/P^{P2H}_{h,Min}$	30MW / 10MW
	C^{SU}_{h}/C^{SD}_{h}	30MW/20MW		$P^{H2P}_{h,Max}/P^{H2P}_{h,Min}$	30MW / 10MW
	T^{Ue}_{h}/T^{De}_{h}	1(h)/1(h)		$\eta^{P2H}_{h}/\eta^{H2P}_{h}$	0.80 / 0.75
	η^{CHP}_{h}	0.35	GS	$GS^{Max}_{h}/GS^{Min}_{h}$	300Kcf / 1800Kcf
TES	B^{Max}_{h}/B^{Min}_{h}	180MW / 10MW		$GS^{ch,max}_{h}/GS^{dis,max}_{h}$	3000Kcf / 3000Kcf
	$H^{ch}_{h,Max}/H^{dis}_{h,Max}$	30MW / 30MW		$\eta^{GSS,ch}_{h}/\eta^{GSS,dis}_{h}$	0.9 / 0.9
	$\eta^{ch}_{h}/\eta^{dis}_{h}$	0.95 / 0.95		$GS_{h,s,t=0}/GS_{h,s,t=24}$	310Kcf
	$B^{Max}_{h,s,t=1}/B^{Min}_{h,s,t=24}$	30MW	EB	η^{EB}_{h}	2
MESO	$P^{EH,Max}_{h}/P^{EH,Min}_{h}$	150MW /-150MW		$P^{EB,max}_{h}$	20MW

References

[1] S. Zeynali, N. Rostami, M. R. Feyzi, Multi-objective optimal short-term planning of renewable distributed generations and capacitor banks in power system considering different uncertainties including plug-in electric vehicles, International Journal of Electrical Power and Energy Systems 119 (2020) 105885. doi:10.1016/j.ijepes.2020.105885.

[2] H. Abid, J. Thakur, D. Khatiwada, D. Bauner, Energy storage integration with solar pv for increased electricity access: A case study of burkina faso, Energy (2021) 120656.

[3] S. Arango-Aramburo, S. Bernal-García, E. R. Larsen, Renewable energy sources and the cycles in deregulated electricity markets, Energy 223 (2021) 120058.

[4] V. Halmschlager, R. Hofmann, Assessing the potential of combined production and energy management in industrial energy hubs–analysis of a chipboard production plant, Energy 226 (2021) 120415.

[5] J. Zhang, Y. Zhou, Z. Li, J. Cai, Three-level day-ahead optimal scheduling framework considering multi-stakeholders in active distribution networks: Up-to-down approach, Energy 219 (2021) 119655. doi:10.1016/j.energy.2020.119655.

[6] X. Li, W. Wang, H. Wang, A novel bi-level robust game model to optimize a regionally integrated energy system with large-scale centralized renewable-energy sources in western china, Energy (2021) 120513.

[7] M. Liu, S. Wang, J. Yan, Operation scheduling of a coal-fired chp station integrated with power-to-heat devices with detail chp unit models by particle swarm optimization algorithm, Energy 214 (2021) 119022. doi:10.1016/j.energy.2020.119022.

[8] M. Liu, M. Liu, Y. Wang, W. Chen, J. Yan, Thermodynamic optimization of coal-fired combined heat and power (chp) systems integrated with steam ejectors to achieve heat–power decoupling, Energy (2021) 120707.

[9] I. Iliev, A. Terziev, H. Beloev, I. Nikolaev, A. Georgiev, Comparative analysis of the energy efficiency of different types co-generators at large scales chps, Energy 221 (2021) 119755. doi:10.1016/j.energy.2021.119755.

[10] Y. Song, L. Shangguan, G. Li, Simulation analysis of flexible concession period contracts in electric vehicle charging infrastructure public-private-partnership (EVCI-PPP) projects based on Time-of-use (TOU) charging price strategy, Elsevier, 2021.

[11] E. Nasrolahpour, J. Kazempour, H. Zareipour, W. D. Rosehart, A bilevel model for participation of a storage system in energy and reserve markets, IEEE Transactions on Sustainable Energy 9 (2) (2018) 582–598. doi:10.1109/TSTE.2017.2749434.

[12] A. Alabdulwahab, A. Abusorrah, X. Zhang, M. Shahidehpour, Coordination of interdependent natural gas and electricity infrastructures for firming the variability of wind energy in stochastic day-ahead scheduling, IEEE Transactions on Sustainable Energy (2015). doi:10.1109/TSTE.2015.2399855.

[13] M. Thompson, Natural gas storage valuation, optimization, market and credit risk management, Journal of Commodity Markets 2 (1) (2016) 26–44. doi:10.1016/j.jcomm.2016.07.004.

[14] X. Yang, Z. Chen, X. Huang, R. Li, S. Xu, C. Yang, Robust capacity optimization methods for integrated energy systems considering demand response and thermal comfort, Energy 221 (2021) 119727. doi:10.1016/j.energy.2020.119727.

[15] S. F. Afzali, V. Mahalec, Optimal design, operation and analytical criteria for determining optimal operating modes of a cchp with fired hrsg, boiler, electric chiller and absorption chiller, Energy 139 (2017) 1052–1065. doi:10.1016/j.energy.2017.08.029.

[16] X. Zhang, M. Shahidehpour, A. Alabdulwahab, A. Abusorrah, Multiple energy infrastructures, IEEE Transactions on Smart Grid (2015) 1–10.

[17] M. Moeini-Aghtaie, H. Farzin, M. Fotuhi-Firuzabad, R. Amrollahi, Generalized analytical approach to assess reliability of renewable-based energy hubs, IEEE Transactions on Power Systems 32 (1) (2017) 368–377. doi:10.1109/TPWRS.2016.2549747.

[18] M. Yan, Y. He, M. Shahidehpour, X. Ai, Z. Li, J. Wen, Coordinated regional-district operation of integrated energy systems for resilience en-

hancement in natural disasters, IEEE Transactions on Smart Grid (2018). doi:10.1109/TSG.2018.2870358.

[19] M. Mohammadi, Y. Noorollahi, B. Mohammadi-ivatloo, M. Hosseinzadeh, H. Yousefi, S. T. Khorasani, Optimal management of energy hubs and smart energy hubs – a review, Renewable and Sustainable Energy Reviews 89 (February) (2018) 33–50. doi:10.1016/j.rser.2018.02.035.

[20] M. Mohammadi, Y. Noorollahi, B. Mohammadi-ivatloo, H. Yousefi, S. Jalilinasrabady, Optimal scheduling of energy hubs in the presence of uncertainty-a review, Journal of Energy Management and Technology 1 (1) (2017) 1–17. doi:10.22109/jemt.2017.49432.

[21] V. Davatgaran, M. Saniei, S. S. Mortazavi, Optimal bidding strategy for an energy hub in energy market, Energy (2018). doi:10.1016/j.energy.2018.01.174.

[22] T. Zhao, X. Pan, S. Yao, C. Ju, L. Li, Strategic bidding of hybrid ac/dc microgrid embedded energy hubs: A two-stage chance constrained stochastic programming approach, IEEE Transactions on Sustainable Energy 11 (1) (2020) 116–125. doi:10.1109/TSTE.2018.2884997.

[23] A. Najafi, A. Tavakoli, M. Pourakbari-Kasmaei, M. Lehtonen, A risk-based optimal self-scheduling of smart energy hub in the day-ahead and regulation markets, Journal of Cleaner Production 279 (2021) 123631. doi:10.1016/j.jclepro.2020.123631.

[24] S. Khazeni, A. Sheikhi, M. Rayati, S. Soleymani, A. M. Ranjbar, Retail market equilibrium in multicarrier energy systems: A game theoretical approach, IEEE Systems Journal 13 (1) (2019) 738–747. doi:10.1109/JSYST.2018.2812807.

[25] E. G. Tsimopoulos, M. C. Georgiadis, Nash equilibria in electricity pool markets with large-scale wind power integration, Energy (2021) 120642.

[26] A. Nikpour, A. Nateghi, M. Shafie-khah, J. P. Catalão, Day-ahead optimal bidding of microgrids considering uncertainties of price and renewable energy resources, Energy (2021) 120476.

[27] A. Heidari, S. S. Mortazavi, R. C. Bansal, Equilibrium state of a price-maker energy hub in a competitive market with price uncertainties, IET Renewable Power Generation 14 (6) (2020) 976–985. doi:10.1049/iet-rpg.2019.0958.

[28] A. Najafi, H. Falaghi, J. Contreras, M. Ramezani, A stochastic bilevel model for the energy hub manager problem, IEEE Transactions on Smart Grid 8 (5) (2017) 2394–2404. doi:10.1109/TSG.2016.2618845.

[29] M. Z. Oskouei, M. A. Mirzaei, B. Mohammadi-Ivatloo, M. Shafiee, M. Marzband, A. Anvari-Moghaddam, A hybrid robust-stochastic approach to evaluate the profit of a multi-energy retailer in tri-layer energy markets, Energy 214 (2021) 118948.

[30] W. Hui, Z. Xin-gang, R. Ling-zhi, L. Fan, An agent-based modeling approach for analyzing the influence of market participants' strategic behavior on green certificate trading, Energy 218 (2021) 119463.

[31] R. Li, W. Wei, S. Mei, Q. Hu, Q. Wu, Participation of an energy hub in electricity and heat distribution markets: An mpec approach, IEEE Transactions on Smart Grid (2019). doi:10.1109/TSG.2018.2833279.

[32] N. Nasiri, A. Sadeghi Yazdankhah, M. A. Mirzaei, A. Loni, B. Mohammadi-Ivatloo, K. Zare, M. Marzband, A bi-level market-clearing for coordinated regional-local multi-carrier systems in presence of energy storage technologies, Sustainable Cities and Society 63 (2020) 102439. doi:10.1016/j.scs.2020.102439.

[33] M. Yazdani-Damavandi, N. Neyestani, G. Chicco, M. Shafie-Khah, J. P. Catalão, Aggregation of distributed energy resources under the concept of multienergy players in local energy systems, IEEE Transactions on Sustainable Energy 8 (4) (2017) 1679–1693. doi:10.1109/TSTE.2017.2701836.

[34] M. Yazdani-Damavandi, N. Neyestani, M. Shafie-khah, J. Contreras, J. P. S. Catalao, Strategic behavior of multi-energy players in electricity markets as aggregators of demand side resources using a bi-level approach, IEEE Transactions on Power Systems 33 (1) (2017) 397–411. doi:10.1109/tpwrs.2017.2688344.

[35] A. Mirzapour-kamanaj, M. Majidi, K. Zare, R. Kazemzadeh, Electrical power and energy systems optimal strategic coordination of distribution networks and interconnected energy hubs : A linear multi-follower bi-level optimization model, Electrical Power and Energy Systems 119 (February) (2020) 105925. doi:10.1016/j.ijepes.2020.105925.

[36] P. Sheikhahmadi, S. Bahramara, The participation of a renewable energy-based aggregator in real-time market: A bi-level approach, Journal of Cleaner Production 276 (2020) 123149. doi:10.1016/j.jclepro.2020.123149.

[37] A. Mansour-Saatloo, M. Agabalaye-Rahvar, M. A. Mirzaei, B. Mohammadi-Ivatloo, M. Abapour, K. Zare, Robust scheduling of hydrogen based smart micro energy hub with integrated demand response, Journal of Cleaner Production 267 (2020) 122041. doi:10.1016/j.jclepro.2020.122041.

[38] A. Mansour-Saatloo, M. A. Mirzaei, B. Mohammadi-Ivatloo, K. Zare, A risk-averse hybrid approach for optimal participation of power-to-hydrogen technology-based multi-energy microgrid in multi-energy markets, Sustainable Cities and Society 63 (2020) 102421. doi:10.1016/j.scs.2020.102421.

[39] M. A. Mirzaei, M. Hemmati, K. Zare, M. Abapour, B. Mohammadi-Ivatloo, M. Marzband, A. Anvari-Moghaddam, A novel hybrid two-stage framework for flexible bidding strategy of reconfigurable micro-grid in day-ahead and real-time markets, International Journal of Electrical Power and Energy Systems 123 (June) (2020) 106293. doi:10.1016/j.ijepes.2020.106293.

[40] H. Nasiraghdam, A. Safari, Techno-economic assessment of combined power to hydrogen technology and hydrogen storage in optimal bidding strategy of high renewable units-penetrated microgrids, Sustainable

Energy Technologies and Assessments 42 (September) (2020) 100832. doi:10.1016/j.seta.2020.100832.

[41] G. Pan, W. Gu, Y. Lu, H. Qiu, S. Lu, S. Yao, Accurate modeling of a profit-driven power to hydrogen and methane plant toward strategic bidding within multi-type markets, IEEE Transactions on Smart Grid 12 (1) (2021) 338–349. doi:10.1109/TSG.2020.3019043.

[42] A. Mansour-Saatloo, M. Agabalaye-Rahvar, M. A. Mirzaei, B. Mohammadi-Ivatloo, M. Abapour, K. Zare, Robust scheduling of hydrogen based smart micro energy hub with integrated demand response, Journal of Cleaner Production 267 (2020) 122041.

[43] M. A. Mirzaei, M. Z. Oskouei, B. Mohammadi-Ivatloo, A. Loni, K. Zare, M. Marzband, M. Shafiee, Integrated energy hub system based on power-to-gas and compressed air energy storage technologies in the presence of multiple shiftable loads, IET Generation, Transmission and Distribution 14 (13) (2020) 2510–2519. doi:10.1049/iet-gtd.2019.1163.

[44] M. A. Mirzaei, A. Sadeghi Yazdankhah, B. Mohammadi-Ivatloo, Stochastic security-constrained operation of wind and hydrogen energy storage systems integrated with price-based demand response, International Journal of Hydrogen Energy (2019). doi:10.1016/j.ijhydene.2018.12.054.

[45] S. Zeynali, N. Rostami, A. Ahmadian, A. Elkamel, Robust multi-objective thermal and electrical energy hub management integrating hybrid battery-compressed air energy storage systems and plug-in-electric-vehicle-based demand response, Journal of Energy Storage 35 (2021) 102265. doi:10.1016/j.est.2021.102265.

[46] D. Bertsimas, M. Sim, Robust discrete optimization and network flows, Vol. 98, Springer, 2003, pp. 49–71. doi:10.1007/s10107-003-0396-4.

[47] M. A. Mirzaei, M. N. Heris, K. Zare, B. Mohammadi-ivatloo, M. Marzband, S. Asadi, A. Anvari-moghaddam, Evaluating the impact of multi-carrier

energy storage systems in optimal operation of integrated electricity , gas and district heating networks, Applied Thermal Engineering (2020) 115413doi:10.1016/j.applthermaleng.2020.115413.

[48] P. Sheikhahmadi, S. Bahramara, A. Mazza, G. Chicco, J. P. Catalão, Bi-level optimization model for the coordination between transmission and distribution systems interacting with local energy markets, International Journal of Electrical Power & Energy Systems 124 (2021) 106392.

[49] M. A. Mirzaei, M. Z. Oskouei, B. Mohammadi-Ivatloo, A. Loni, K. Zare, M. Marzband, M. Shafiee, Integrated energy hub system based on power-to-gas and compressed air energy storage technologies in the presence of multiple shiftable loads, IET Generation, Transmission & Distribution 14 (13) (2020) 2510–2519.

[50] S. Zeynali, N. Rostami, A. Ahmadian, A. Elkamel, Two-stage stochastic home energy management strategy considering electric vehicle and battery energy storage system: An ann-based scenario generation methodology, Sustainable Energy Technologies and Assessments 39 (2020) 100722. doi:10.1016/j.seta.2020.100722.

[51] A. J. Conejo, M. Carrión, J. M. Morales, et al., Decision making under uncertainty in electricity markets, Vol. 1, Springer, 2010.